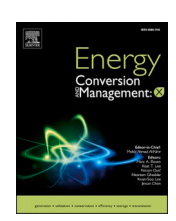
FISEVIER

Contents lists available at ScienceDirect

## Energy Conversion and Management: X

journal homepage: www.sciencedirect.com/journal/energy-conversion-and-management-x





# Carbon negative transportation fuels – A techno-economic-environmental analysis of biomass pathways for transportation

Micah Jasper<sup>a,\*</sup>, Navid Rafati<sup>a</sup>, Keith Schimmel<sup>b</sup>, Abolghasem Shahbazi<sup>a</sup>, Fanxing Li<sup>c</sup>, Mark Mba-Wright<sup>d</sup>, Lijun Wang<sup>a</sup>

- <sup>a</sup> North Carolina Agricultural and Technical State University, Greensboro, NC, USA
- <sup>b</sup> Olivet Nazarene University, Bourbonnais, IL, USA
- c North Carolina State University, Raleigh, NC, USA
- <sup>d</sup> Iowa State University, Ames, IA, USA

#### ARTICLE INFO

Keywords:
Fischer-Tropsch
Biofuel
Biomass gasification
Aspen Plus
Process modeling
Techno-economic analysis
Life-cycle assessment
LCA
TEA
GaBi
Biorefinery

#### ABSTRACT

Global warming and fossil fuel depletion have necessitated alternative sources of energy. Biomass is a promising fuel source because it is renewable and can be carbon negative, even without carbon capture and storage. This study considers biomass as a clean, renewable source for transportation fuels. An Aspen Plus process simulation model was built of a biomass gasification biorefinery with Fischer-Tropsch (FT) synthesis of liquid fuels. A GaBi life cycle assessment model was also built to determine the environmental impacts using a cradle-to-grave approach. Three different product pathways were considered: Fischer-Tropsch synthetic diesel, hydrogen, and electricity. An offgas autothermal reformer with a recycle loop was used to increase FT product yield. Different configurations and combinations of biorefinery products are considered. The thermal efficiency and cost of production of the FT liquid fuels are analyzed using the Aspen Plus process model. The greenhouse gas emissions, profitability, and mileage per kg biomass were compared. The mileage traveled per kilogram biomass was calculated using modern (2019-2021) diesel, electric, and hydrogen fuel cell vehicles. The overall thermal efficiency was found to be between 20 and 41% for FT fuels production, between 58 and 61% for hydrogen production, and around 25-26% for electricity production for this biorefinery. The lowest production costs were found to be \$3.171/gal of FT diesel (\$24.304/GJ), \$1.860/kg of H<sub>2</sub> (\$15.779/GJ), and 13.332¢/kWh for electricity (\$37.034/GJ). All configurations except one had net negative carbon emissions over the life cycle of the biomass. This is because carbon is absorbed in the trees initially, and some of the carbon is sequestered in ash and unconverted char from the gasification process, furthermore co-producing electricity while making transportation fuel offsets even more carbon emissions. Compared to current market rates for diesel, hydrogen, and electricity, the most profitable biorefinery product is shown to be hydrogen while also having net negative carbon emissions. FT diesel can also be profitable, but with a slimmer profit margin (not considering government credits) and still having net negative carbon emissions. However, our biorefinery could not compete with current commercial electricity prices in the US. As oil, hydrogen, and electricity prices continue to change, the economics of the biorefinery and the choice product will change as well. For our current biorefinery model, hydrogen seems to be the most promising product choice for profit while staying carbon negative, while FT diesel is the best choice for sequestering the most carbon and still being profitable.

Abbreviations: FT, Fischer-Tropsch; CCUS, carbon capture, utilization, and storage; GTL, gas-to-liquids; CTL, coal-to-liquids; BTL, biomass-to-liquids; BTH, biomass-to-hydrogen; LHV, lower heating value; HHV, higher heating value; AGR, acid gas removal; ATR, autothermal reforming; GHG, greenhouse gas; LCA, life cycle assessment; WGS, water-gas shift; FB, fluidized bed; FCC, fluid catalytic cracking; ASF, Anderson-Schulz-Flory product distribution model; TCI, total capital investment; GGE, gallon of gasoline equivalent; CEPCI, Chemical Engineering Plant Cost Index; FTL, Fischer-Tropsch liquids; O&M, operation and maintenance; OT, once-through; GTG, gate-to-gate; WTW, wheel-to-well; CTG, cradle-to-grave.

E-mail address: mnjasper@aggies.ncat.edu (M. Jasper).

<sup>\*</sup> Corresponding author.

#### Introduction

There is an ever-increasing demand for the production of clean and renewable energy, because of the depletion of fossil fuels and global warming. In the US, the Energy Independence and Security Act of 2007 aims for the production of 36 billion US gallons of biofuels annually by 2022 [1]. Converting biomass into liquids fuels (e.g., synthetic diesel, gasoline, jet fuel) by integrating gasification and Fischer-Tropsch (FT) synthesis is a promising and potentially carbon negative [2-4] process without the need for carbon capture, utilization, and storage (CCUS). FT synthesis is a proven technology for producing liquid fuels such as diesel, gasoline, and kerosene from syngas in the presence of a catalyst, usually cobalt-based or iron-based. Syngas is most often produced from coal gasification but can also be produced from natural gas reforming and biomass gasification. There are several commercial plants around the world currently producing FT fuels from natural gas (gas-to-liquid, GTL) [5,6] and coal (coal-to-liquid, CTL) [7,8]. Production of liquid FT fuels from biomass (biomass-to-liquid, BTL) is not as established commercially, though there are pilot plants and demonstration facilities around the world [9], and many co-fired coal and biomass gasification facilities. The largest obstacle for FT liquid fuels from biomass is that it is not economical in today's energy market, mostly because of high capital cost and low crude oil and natural gas prices [10].

FT biofuels have many advantages over other more common biofuels, such as bioethanol or biodiesel, because:

- 1. FT liquids can be produced from non-food crops and waste streams, like wood, residues, grasses, lignocellulosic biomass, etc.
- They have the same composition as conventional petroleum based transportation fuels, diesel and gasoline, but have almost no sulfur content, and no need to blend with petroleum based fuels.
- 3. Furthermore, FT liquids are compatible with current automobile engines and the fuel infrastructure for distribution and storage, because They are nearly identical to petroleum fuels.

The FT synthesis process can convert syngas into various fuels and chemicals such as gasoline, diesel, kerosene, methanol, ethanol, paraffins, and olefins [6,11–13]. The FT process can be divided into four main stages: (1) syngas production (e.g., gasification or reforming), (2) syngas cleaning and conditioning, (3) FT synthesis, (4) FT product refining and upgrading. For the first stage, syngas can be produced in many ways depending on the feedstock: gasification of coal, petroleum coke, biomass, or municipal solid waste (MSW), or reforming of natural gas. In stage two, syngas requires cleaning to remove contaminants such as particulates, sulfur, and nitrogen containing compounds. The syngas for FT synthesis will likely require the H<sub>2</sub>/CO ratio to be adjusted for the desired products, usually the CO2 content is reduced [14]. At stage three, the cleaned and conditioned syngas is catalytically converted to hydrocarbon chains in a FT synthesis reactor. The FT products are then separated and upgraded into different liquid fuels and chemicals just like in a petroleum refinery [15].

There are many studies reviewing the technical and economic aspects of biomass-to-liquids (BTL) processes [2,16]. Tijmensen et al. [17] found that the thermal efficiency of a BTL process using the lower heating value (LHV) was between 33 and 40% for gasification at atmospheric pressure and between 42 and 50% for pressurized gasification systems. Hamelinck at al. [18] reported similar efficiencies between 40 and 45% bases on the higher heating value (HHV). The production costs of FT liquids from biomass have in the past been found to be 2–4 times higher than conventional diesel from petroleum [17,18]. Leibbrandt et al. [19] found that a steam gasification process with a moderate steam-to-biomass ratio followed by a WGS reactor was more

efficient than operating the gasifier with a high steam-to-biomass ratio and no WGS reactor.

Biomass-to-hydrogen (BTH) is a promising pathway that is gaining increased attention [20–22]. It has the potential to be carbon negative much like FT diesel production [23], even without CCUS. Currently, 95% of hydrogen comes from fossil fuels. Grey hydrogen is produced from fossil fuels without CCUS and has production costs ranging from 1 to 3 \$/kg H<sub>2</sub>. At the US Gulf coast grey hydrogen costs \$1.25 \$/kg and \$2/kg in California [24]. Blue hydrogen produced form fossil fuels but with CCUS is produced for around 1.9 \$/kg in the Netherlands. Green hydrogen which is produced from electricity or renewable energy is priced at around \$4.3/kg. However, a report from the California Energy Commission found that the average price for hydrogen for fuel cell vehicles was \$16.51/kg at the pump [25]. Also, hydrogen fueling stations are very remote. In the US and Canada, there are currently only hydrogen fueling stations in California, Hawaii, and Vancouver and Quebec [26].

Many of the fundamental biorefinery processes for hydrogen production are similar to FT production. However, in hydrogen production, the syngas must be shifted using steam to obtain a raw hydrogen stream which is mainly comprised of hydrogen and carbon dioxide. The carbon dioxide is typically separated using conventional acid gas removal (AGR) processes followed by the recovery of high purity hydrogen (99.97% or higher by volume) in a pressure swing adsorption (PSA) system [27]. Our refinery is based on the autothermal reforming (ATR) technology which is the most cost effective technology for hydrogen production from gaseous hydrocarbons.

This research compares different objectives for deciding which biorefinery configuration to build or which product to target. The most obvious objectives are profitability and greenhouse gas (GHG) emissions. A robust life cycle assessment (LCA) will include many other environmental objectives in addition to GHG emissions, such as human toxicity, acidification, water and soil ecotoxicity, land use changes, and many more, but these are not considered here. One objective that is not often considered is miles traveled per kg of fuel. Using modern passenger car models—a 2019 Chevy Cruise, 2021 Honda Clarity, and a 2021 Tesla Model S—we calculated the miles traveled per kg of biomass. These different objectives profitability, GHG emissions, and transportation miles are contrasted for different biorefinery configurations.

#### Methodology

Process model development

There can be many possible configurations of BTL conversion depending on the type of feedstock pretreatment, gasification technology, syngas cleaning and treatment, and FT synthesis. Biomass feedstock is first sent through pretreatment processes of crushing, shredding, griding and drying to reduce the size and moisture in the biomass. The biomass particles are then gasified which is a partial combustion process controlling the oxygen and temperature to ensure the biomass is converted into syngas instead of full combustion. Then the syngas is cleaned and conditioned in several steps to prepare it for FT synthesis or hydrogen separation, including removal of particulates, removal of nitrogen and sulfur compounds, removal and/or catalytic cracking of tar components, water-gas shift (WGS) to adjust the H2/CO ratio, and CO2 removal. In the FT processes, the prepared syngas then enters a FT reactor which typically includes an iron or cobalt catalyst and operates at various temperatures and pressures depending on the desired FT products. A nickel catalyst is possible, but Ni favors methane synthesis (methanation) and therefore is not typically used [28]. Rhodium and ruthenium are also possible FT catalysts, but they are very expensive and

are therefore not used in industry [29–31]. After FT synthesis, the effluent is cooled to separate the liquid hydrocarbons ( $C_{5+}$ ) from the offgas (unconverted reactants and  $C_1$ - $C_4$  hydrocarbons). The offgas can be combusted to generate heat and/or electricity or it can be recycled in a separate reforming reactor to convert it back into syngas and then back into the FT reactor. Finally, the liquid FT products can be upgraded and separated, just like in an oil refinery, into diesel, gasoline and other fuels.

This research studies an integrated process configuration consisting of gasification, water–gas shift (WGS), acid-gas removal (AGR), FT synthesis, FT offgas and methane autothermal reforming (ATR), and power generation. These processes are modeled in Aspen Plus as shown in Fig. 1. Previous studies demonstrate that a thermal loading higher than 400 MW $_{\rm th}$  is required for economic FT production [18,19] and thus in this study, the biomass input is fixed at 400 MW $_{\rm th}$  LHV. This corresponds to 1920 tonne/day of dried woody biomass with 15% moisture content. The design and specifications of the plant process stages are described in the following sections.

#### Gasification

Fig. 2 shows the process flowchart developed in Aspen Plus. There are many types of gasifiers: downdraft, updraft, moving bed, entrained flow, etc. This research uses a fluidized bed gasifier, because it can accept a wide range of feedstock. The fluidized bed gasifier has been modeled using the sequential modular two-phase model described mathematically in [32,33] and demonstrated in [34,35]. Most fluidized beds are either circulating fluidized beds or bubbling fluidized beds depending on the configuration of the reactor and velocity of the gas entering the reactor. Fluidized beds vigorously mix solids and gas and therefore have high reaction rates and heat and mass transfer rates [36]. Fluidized beds can also use catalytic particles as the bed material like dolomite and spent fluid catalytic cracking (FCC) catalyst to help improve tar cracking. In fact when FCC catalyst is added to the bed material it produced syngas with very low tar content and eliminated the need for a additional tar cracking reactor [37]. Successful pilot plant and commercial scale gasifiers include Stein, IGT, EPI, TPS, BCL, and Sydkraft gasifiers [36].

This study uses a pressurized, oxygen blown fluidized bed gasifier described in [35]. Previous studies have shown that using oxygen instead of air as the gasifying agent has promising economics and many advantages for subsequent FT liquid fuel synthesis [18,19]. When using air in the gasifier, a large amount of nitrogen is introduced in the system, this reduces the molar fraction of the  $\rm H_2$  and CO and reduces the yields of the FT hydrocarbons produces in the FT reactor and also increases the size required for the equipment, it also leads to  $\rm NO_x$  byproducts which cause pollutions and unwanted effects in the FT reactor.

Process simulation software has typically not included built-in unit processes to model the complicated kinetics and hydrodynamics in a fluidized bed (FB) reactor. The two-phase model described by Kunii and Levenspiel [38] is a mathematical description of the dynamics occurring in FB systems. The sequential modular two-phase model or sequential modular simulation (SMS) was developed [32] to adapt the

mathematical two-phase model to process simulators. However, recent additions of Aspen Plus have a built-in unit process for FB reactors included in the solids package. This model specifically accounts for the hydrodynamics of a bubbling bed.

The biomass feedstock is raw pine sawdust with the composition taken from [39]. The energy density of the biomass feedstock is assumed to be 18 MJ/kg LHV from the GREET database [40]. We assume that 8.5% of the weight of the biomass is taken out of the gasifier in mineral ash and unreacted char. The biomass is assumed to have 30% moisture, which is dried down to 15% using waste heat from steam. For the biomass input of 1920 tonne/day (400 MWth LHV), 26.2 MW of thermal power is required to evaporate the 15% moisture. After drying the biomass enters the gasifier. Drying and devolatilization (primary pyrolysis) are the first stage of transformation inside of the gasifier. In Aspen Plus, this is modeled as a separate unit process even though it happens inside of the physical gasifier. This is assumed to happen instantaneously as the biomass enters the gasifier. The gasification model is described in another paper [34]. The simulation was validated using experimental data from the IGT gasifier using design parameters from [41]. Table 1 gives the basic mass and energy flows of the gasifier. All configurations of the biorefinery use the same biomass feedstock and the same syngas composition which are given in Table 2. The steam-tobiomass ratio (STB) used in the gasifier was 0.3 kg steam/kg biomass. We also used oxygen from an on-site cryogenic oxygen separator. The ratio of O2 to biomass (OTB)was also 0.3 kg O2/kg biomass.

#### Gas cleaning

Crude syngas, the untreated syngas exiting the gasifier, may contain many different kinds of contaminants such as particulates, tar and alkali compounds, sulfur, nitrogen and chlorine compounds (H2S, COS, HCN, NH<sub>3</sub>, NO<sub>x</sub>, HCl, etc.) depending on the type of biomass and the operating condition of the gasifier. These contaminants can foul the FT reactor and other downstream equipment as well as cause erosion and corrosion problems if not effectively removed [42]. Contaminants will also pollute the hydrogen product gas in the hydrogen configurations. Contaminants also lower the activity of the catalysts used in the downstream processes: the WGS reactor, the FR reactor, the ATR reactor [43]. Sulfur poisons iron and cobalt FT catalysts by preferentially adsorbing to the active sites of the catalysts [44,45]. Therefore, syngas needs to go through several cleaning and conditioning steps to reduce the contaminants. Wet and dry cleaning are two types of cleaning methods commonly used. Wet syngas cleaning is commonly used in industry, while dry cleaning is still being improved. Hot (dry) syngas cleaning may prove to be more efficient thermally because it does not require cooling before cleaning, but it is still not commonly used on a large scale commercially. Therefore, wet syngas cleaning is used in this study as described by [46]. First, particulates are removed in a cyclone (or series of cyclones), then the syngas is cooled to below 100 °C and contacted with scrubbing fluids such as water or a NaOH solution to remove nitrogen contaminants (NH<sub>3</sub>, HCN) and tars [42]. The number and type of wet scrubbers and filters can be adjusted to the type and amount of contaminants in the syngas to suit the downstream processes.

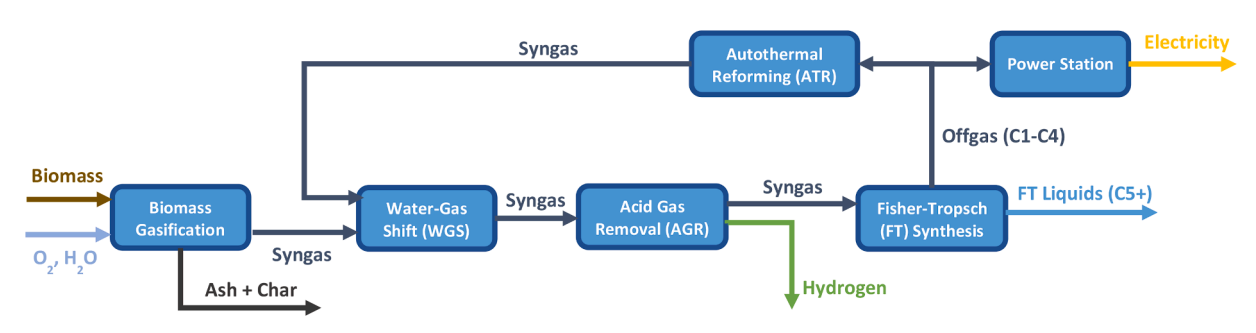
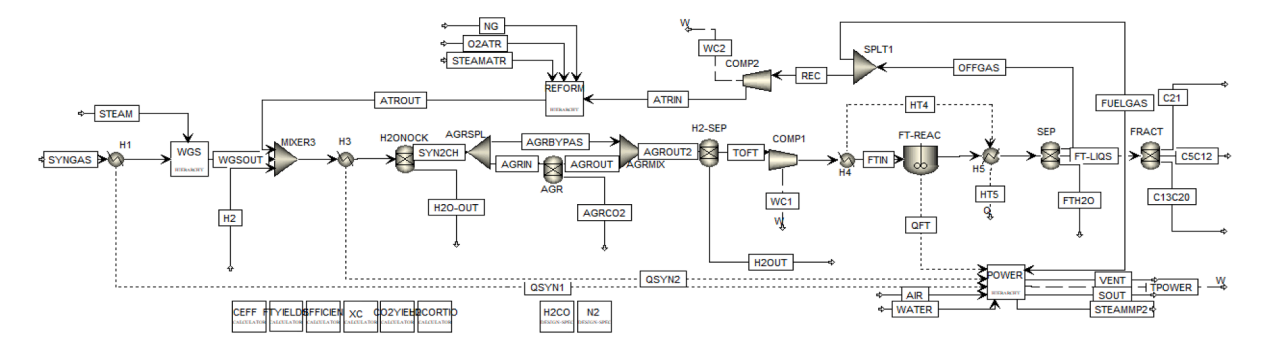
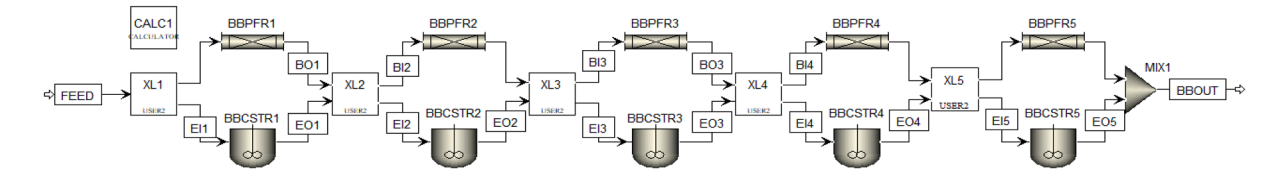


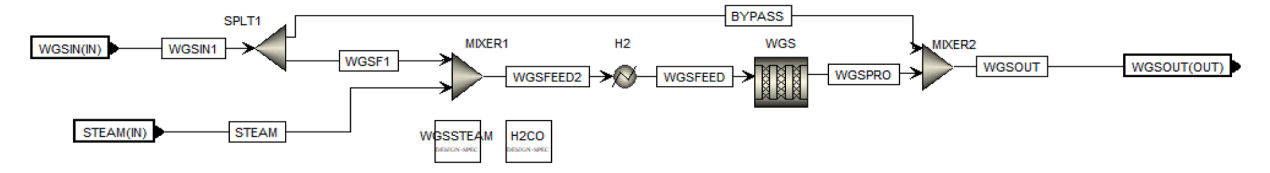
Fig. 1. Flowsheet of Biorefinery Process Model (400 MW<sub>th</sub> LHV).



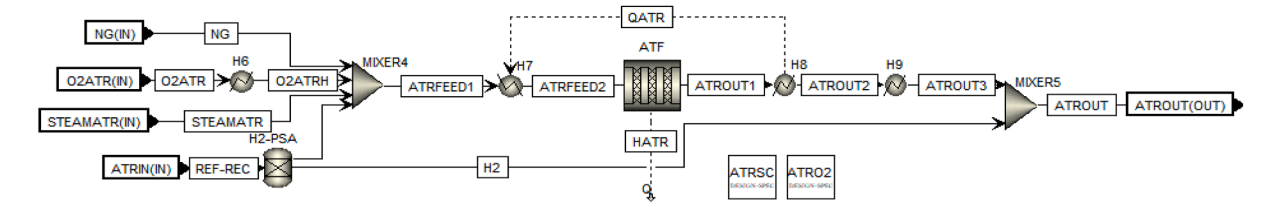
## a. Process Flow Diagram for the Overall Biorefinery



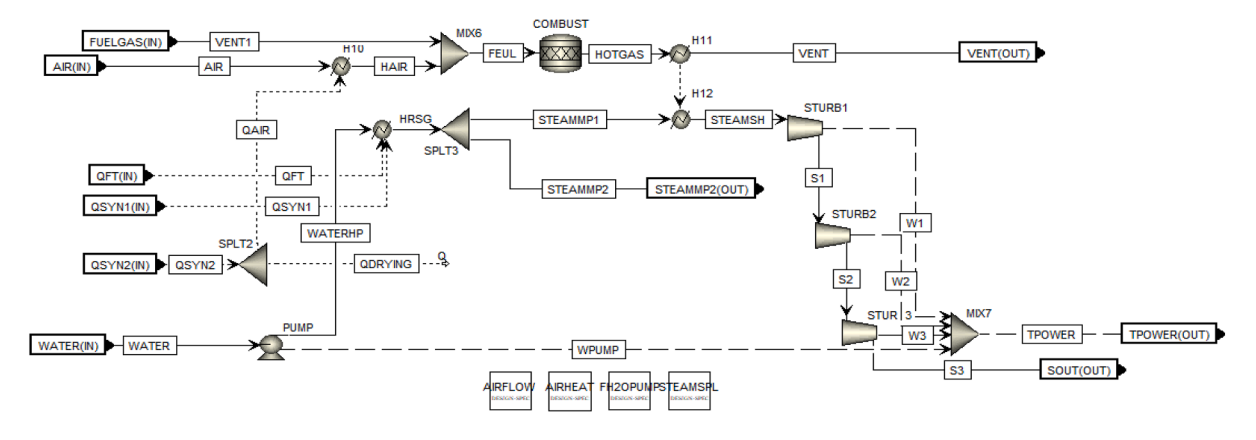
## b. Subprocess Flowsheet for the Bubbling Fluidized Bed Biomass Gasification model [35]



#### c. Subprocess Flowsheet for the Water Gas Shift Reactor



#### d. Subprocess Flowsheet for Offgas and Natural Gas Reformer



## e. Subprocess Flowsheet for Heat Recovery and Power Generation

Fig. 2. Process Flow Diagram developed in Aspen Plus for Biomass Gasification Biorefinery with FT Synthesis and Electricity Generation.

 Table 1

 Gasifier Inflows and Outflows Used in Simulation [34].

Inflow		Unit
Biomass	22.22	kg/s
Steam (STB $= 0.3$ )	6.67	kg/s
$O_2 (OTB = 0.3)$	6.67	kg/s
Total	35.56	kg/s
Biomass LHV	18	MJ/kg
Biomass Energy LHV	400	MW
Outflow		
Syngas	32.54	kg/s
Ash (8.5%)	3.02	kg/s
Total	35.56	kg/s
Syngas LHV	8.2	MJ/kg
Syngas Energy LHV	266.8	MW
Gasifier Efficiency/CCE	66.7%	

**Table 2** Syngas Composition Used in Simulation [34].

Component	Volume %
CO	22.1%
$CO_2$	20.6%
$H_2$	19.9%
$H_2O$	28.5%
CH <sub>4</sub>	8.9%

Water-Gas shift (WGS)

The  $H_2/CO$  ratio of the syngas is a very important parameter affecting the performance of the FT process. The optimal  $H_2/CO$  ratio and FT reactor temperature depend on the catalyst and also the desired products. An optimal value for the  $H_2/CO$  ratio reported for low-temperature iron FT synthesis is 1.65 [14]. The  $H_2/CO$  ratio can be adjusted in a WGS reactor unit before entering the FT reactor. WGS usually uses steam to increase the  $H_2$  content in the syngas according to the water–gas shift reaction:

$$CO + H_2O \leftrightarrow CO_2 + H_2 \tag{1}$$

For the WGS reactor, a sour water–gas shift (SWGS) process (also called sulfur resistant shift or sour shift) is used. The SWGS usually uses a cobalt-molybdenum combined catalyst because it is resistant to sulfur poisoning. The sour shift is more commonly used for coal applications than the alternative high or low temperature sweet shift. The sour shift

 $\label{eq:carbon number n} \textbf{Table 3} \\ \textbf{Carbon number n, mole fractions } m_n \text{ and kinetic constants } k_n \text{ for the FT synthesis reaction for the paraffin hydrocarbons studied.}$ 

n	Symbol	m <sub>n</sub>	k <sub>n</sub>
1	CH <sub>4</sub>	0.33333	18.533
2	$C_2H_6$	0.22222	12.356
3	$C_3H_8$	0.14815	8.237
4	$C_4H_{10}$	0.09877	5.491
5	$C_5H_{12}$	0.06584	3.661
6	$C_6H_{14}$	0.04390	2.441
7	$C_7H_{16}$	0.02926	1.627
8	$C_8H_{18}$	0.01951	1.085
9	$C_9H_{20}$	0.01301	0.723
10	$C_{10}H_{22}$	0.00867	0.482
11	$C_{11}H_{24}$	0.00578	0.321
12	$C_{12}H_{26}$	0.00385	0.214
13	$C_{13}H_{28}$	0.00257	0.143
14	$C_{14}H_{30}$	0.00171	0.095
15	$C_{15}H_{32}$	0.00114	0.063
16	$C_{16}H_{34}$	0.00076	0.042
17	$C_{17}H_{36}$	0.00051	0.028
18	$C_{18}H_{38}$	0.00034	0.019
19	$C_{19}H_{40}$	0.00023	0.013
20	$C_{20}H_{42}$	0.00015	0.008
23	$C_{23}H_{48}$	0.00030	0.017

process is able to hydrolyze the COS into  $\rm H_2S$  which makes downstream sulfur removal easier [47,48]. In Aspen Plus, a plug flow reactor (PFR) was used for the WGS reactor and the kinetics are given in Table 4. There is a split before the WGS reactor, and the split ratio of the diverted syngas is adjusted using a Design Spec in Aspen Plus to obtain the specified  $\rm H_2/CO$  ratio in the exit syngas. The  $\rm H_2/CO$  ratio can also be adjusted by adding more steam. This is done in the hydrogen configurations.

The syngas exiting the gasifier has a large percentage of  $CO_2$  which will only increase from the WGS reaction. The  $CO_2$  in the syngas will lower the yield of liquid hydrocarbons in FT synthesis for cobalt FT catalysts, but not for iron which we use in our model [49–53]. The Rectisol process is used in this research to remove the  $CO_2$  and other acid gases. This process has a lower energy consumption than other  $CO_2$  removal processes such as Selexol and MDEA [54]. The Rectisol process is capable of removing almost all of the sulfur (down to 0.1 ppmv), but we have configured it to only remove 60% of the  $CO_2$ . Carbon-dioxide in iron FT synthesis inhibits the formation of more  $CO_2$  through the WGS reaction in the FT reactor and thus gives a higher yield of FT product [55]. A zinc oxide guard bed was considered to be used before the FT reactor to remove the sulfur compounds, since the FT catalysts are prone to sulfur poisoning [45].

#### Acid-Gas removal (AGR) and CO2 removal

The Acid-Gas Removal (AGR) system is represented by a Sep1 unit block in Aspen Plus for the sake of simplicity. The syngas enters the AGR unit and two streams exit: the cleaned syngas, and the  $CO_2$  and other undesired contaminants such as  $H_2S$ , water, and tar. The energy cost for the AGR unit was set at a fixed 3.5% of the plants thermal capacity [54], in this case 14 MW, for the Rectisol unit using electricity generated onsite.

Decreasing the amount of  $CO_2$  removed in the AGR process was found to increase the yield of FT liquids in the iron-based FT process. This is because the presence of  $CO_2$  in the FT reactor feed inhibits the WGS reaction with an iron-based FT catalyst [49,50]. This agreed with previous experimental studies that determined that the presence of  $CO_2$  in the syngas fed to an iron-based FT reactor inhibited the generation of additional  $CO_2$  from the WGS reaction [49,50]. An added benefit of reducing the efficiency of the  $CO_2$  removal in the AGR unit, is that it reduces the energy consumption for the unit and thus increases the overall efficiency of the biorefinery further.

#### Fischer-Tropsch (FT) synthesis

The iron-based FT synthesis in this research is operated in low-temperature mode at 240  $^{\circ}\text{C}$  for producing diesel and waxy hydrocarbons [56–58]. The FT reactor type in this research is a slurry phase FT reactor allowing a conversion efficiency of 80% per-pass. Traditional fixed-bed FT reactors only have conversion efficiencies of 40% per pass. Fluidized bed reactors are also used for iron-based FT synthesis, but the fluidized bed was not chosen for this research because there is more economic data for the slurry phase reactor. We assumed the volume of the FT reactor is 2.5  $\text{m}^3$ , the solid loading is 1500 kg, and the particle density is 1957 kg/m³. These are typical properties and catalyst loading in a slurry bubble column FT reactor [18].

The kinetic model for iron-based low temperature FT synthesis is given in the following reaction and kinetic rate expression [56]:

$$nCO + \left(n + \frac{m}{2}\right)H_2 \rightarrow C_nH_m + nH_2O$$
 (2)

$$r_{FT} = k_n \frac{P_{CO} P_{H_2}}{\left(1 + 0.125 P_{CO} + 7.00 P_{H_2O}\right)^2} \left[ \frac{kmol}{kg \cdot s} \right]$$
(3)

where  $r_{FT}$  is the Fischer-Tropsch rate constant for each hydrocarbon considered (only paraffins in this research), and  $P_A$  is the partial pressure of the gas species. The kinetic constant  $k_n$  is different for each hydrocarbon produced and is determined by the Anderson-Schulz-Flory (ASF)

**Table 4**Kinetic Expressions used in the Aspen Plus model.

Reactor	Properties	Reaction	Kinetic Expression	Ref.
WGS (PFR)	N = 26415 $L = 2 m$ $D = 0.01 m$	$CO + H_2O \leftrightarrow CO_2 + H_2$	$r_{WGS} = 2777.78 \exp\left(-\frac{12560}{RT}\right) \left(C_{H_2O}C_{CO} - \frac{C_{H_2}C_{CO_2}}{K_{WGS}}\right) \left[\frac{kmol}{m^3s}\right] K_{WGS} = 0.01702 \exp\left(\frac{37238}{RT}\right)$	[63]
ATR (PFR)	[62] P = 20 bar T = 950 °C V = 208 m <sup>3</sup>	$C_nH_{2n+2} + nO_2 \rightarrow nCO + (n+1)H_2$ $C_nH_{2n+2} + nH_2O \rightarrow nCO + (2n+1)H_2$	$\begin{split} r_{POX} &= (4.6e11 - 2e10 \cdot \mathrm{n}) \mathrm{exp} \bigg( -\frac{125520}{RT} \bigg) C_{C_n H_{2n+2}} C_{O_2} \left[ \frac{kmol}{m^3 s} \right] (\text{for } 1 \leq \mathrm{n} \leq 4) \\ r_{REF} &= 3.0e8 \mathrm{exp} \bigg( -\frac{125520}{RT} \bigg) C_{C_n H_{2n+2}} C_{H_2O} \left[ \frac{kmol}{m^3 s} \right] \end{split}$	[65]
FT (CSTR)	$\begin{split} P &= 20 \text{ bar} \\ T &= 240 \text{ °C} \\ V &= 2.5 \text{ m}^3 \\ W &= 1500 \text{ kg} \\ \rho_p &= 1957 \\ kg/m^3 \end{split}$	$nCO + \left(n + \frac{m}{2}\right)H_2 \rightarrow C_nH_m + nH_2O$ $CO + H_2O \leftrightarrow CO_2 + H_2$	$\begin{split} r_{FT} &= k_n \frac{P_{CO}P_{H_2}}{\left(1 + 0.125P_{CO} + 7.00P_{H_2O}\right)^2} \left[\frac{kmol}{kg \cdot s}\right] k_0 = 55.6 \left[\frac{kmol}{kg \cdot s \cdot MPa^2}\right] \text{(for } k_n \text{ see notes in Section 2.1.5)} \\ r_{FT} &= 1770 \frac{P_{CO}P_{H_2O} - P_{CO_2}P_{H_2}/K_{WGS}}{\left(1 + 2.1P_{CO} + 24.19P_{H_2O}\right)^2} \left[\frac{kmol}{kg \cdot s}\right] K_{WGS} = 0.01702 \text{exp} \left(\frac{37238}{RT}\right) \end{split}$	[56] [56]

product distribution model, which is based on chain growth probabilities [57]. The ASF model calculates the resulting product mole fraction  $m_n$  according to equation 4. Then based on the total CO conversion rate  $k_o$  we are able to calculate the kinetic rate constant for each hydrocarbon  $k_n$  as in equation (5).

$$m_n = \alpha^{n-1}(1-\alpha)$$

$$k_n = m_n \cdot k_0 \tag{5}$$

where  $\alpha$  is the probability of the chain growth and  $m_n$  is the mole fraction of hydrocarbon FT products with n carbon atoms, and  $k_n$  is the kinetic constant for the hydrocarbon number n. The chain growth probability  $\alpha$  has typical ranges of 0.85–0.95 for Ru, 0.70–0.80 for Co, and 0.50–0.70 for Fe [57]. The  $\alpha$  value can be calculated using the empirical correlation given by Song et al. [59], but in this research we have just assumed a fixed value of  $\alpha=0.667$  which is within the normal range for iron. We also assume that paraffins (alkanes) are the only FT products [56–58]. The mole fractions  $m_n$  calculated from the ASF model and the resulting kinetic constants  $k_n$  for each hydrocarbon considered are given in Table 3.

The kinetics and product distribution for the assumed fixed  $\alpha$  value of 0.667 were input as a Langmuir-Hinshelwood-Hougen-Watson (LHHW) reaction in Aspen Plus. The model calculates the syngas conversion and molar yield of hydrocarbons for products up to  $C_{20}$ . The rest of the longer chain hydrocarbons are represented by the cumulative  $C_{\rm N+}$  pseudo chemical. The carbon number that exactly matches the remaining hydrocarbon mole fractions can be calculated as follows:

$$N^{+}(N,\alpha) = N + \frac{1}{1-\alpha} \tag{6}$$

$$m_{N+} = \alpha^N \tag{7}$$

where N + is the carbon number that represents the hydrocarbon products greater than N,  $m_{N+}$  is the combined mole fraction of the hydrocarbons greater than N. Assuming  $\alpha=0.667$  and N = 20, N+ = 23 and  $m_{N+}=3.01\text{e-}4$ . These are also shown in Table 3. The kinetic model for iron-based low temperature FT synthesis and water–gas shift for this specific Aspen Plus implementation is given in Table 4. The iron FT catalyst kinetics are usually reported in literature in moles of CO converted to products per mass of catalyst, which is why the specific

hydrocarbon kinetics must be calculated from a product distribution model. The FT product distribution also varies depending on the catalyst and the FT operating conditions.

#### Autothermal reforming (ATR)

After FT synthesis, products are cooled to separate the gas fraction (unconverted syngas and  $C_1\text{-}C_4$  hydrocarbons) from the liquid and waxes  $(C_{5+})$  and water. The offgas can be recycled or combusted to generate heat and electricity. Since the offgas contains mostly light hydrocarbons, it can be reformed into more syngas and recycled back into the FT reactor to form more liquid FT products. In the ATR reactor, the hydrocarbons react with oxygen and steam to produce  $H_2$  and CO in the following partial oxidation and steam reforming reactions:

$$C_n H_m + \frac{n}{2} O_2 \rightarrow nCO + \frac{m}{2} H_2$$
 (8)

$$C_n H_m + nH_2 O \rightarrow nCO + \left(n + \frac{m}{2}\right) H_2 \tag{9}$$

The autothermal reforming (ATR) reactor is usually operated at higher than 800 °C using a nickel catalyst [60]. In addition to partial oxidation, steam reforming, dry reforming, and the water–gas shift reactions also takes place in the ATR reactor. However, in the Aspen Plus model only partial oxidation and steam reforming are modeled in the ATR reactor. The kinetics for these reactions is given in Table 4.

The oxygen for the ATR unit and is provided by an onsite cryogenic air separation unit (ASU) that provide oxygen at 99.55 purity. The flowrate of  $O_2$  fed into the reformer is controlled in Aspen Plus by a Design Spec to specify the gas outlet temperature at 950 °C. A molar steam to methane ratio is set to 20% above the stoichiometric ratio of 1 to avoid the formation of coke [61]. The energy cost of the ASU unit is set at a fixed 3.8% of the thermal capacity of the plant, in this case 15.2 MW [54].

#### Heat recovery and power generation

Excess heat is used to pre-heat other streams as shown in Fig. 2e. The syngas from the gasifier is cooled in two consecutive heat exchangers before FT synthesis. The first heat exchanger cools the syngas to 350  $^{\circ}\text{C}$  in a vertical fire-tube boiler. The vertical fire-tube boiler minimizes deposition of small particles in the syngas and condensation of alkali species during cooling. The particulates that remain in the syngas after the cyclone are removed by a barrier filter (usually either ceramic or

sintered metal) at 350 °C [2]. In the second syngas cooler, syngas after the WGS reactor and gas exiting the ATR reactor are mixed and cooled to 40 °C. Heat from the first syngas cooler (the fire-tube boiler), and heat from the exothermic FT synthesis reactor are used to generate steam at 250 °C and 20 bar for gasification, ATR, and power generation. Some of the FT offgas is burned in a boiler to produce steam at 510 °C and 70 bar for steam cycle power generation. Air is preheated to 300 °C and fed to the steam boiler using some of the heat recovered from the second heat exchanger. A three-stage steam turbine system was used at lesser pressures of 23.6 bar, 2.4 bar, and 0.046 bar [35]. The isentropic efficiency is set to 0.85 and the mechanical efficiency is 0.98 [17]. Electricity is used onsite and excess electricity is sent to the grid. This study optimizes the design configuration for maximum FT liquids by shifting more offgas to the ATR to be recycled instead of the steam boiler for power generation. This ratio can be adjusted and is set at 24% offgas to the boiler for the FT-E-24 configuration generating a gross electrical power of 55 MW<sub>e</sub>. This ratio can be adjusted to generate more electricity by sending more offgas to the power station or more FT liquids by recycling more offgas to the ATR.

#### Aspen plus simulation

We use Aspen Plus to calculate mass and energy balances and also to provide input to the economic and life cycle assessment (LCA) analyses. The basic input parameters for the Aspen Plus model are described in [35] and further details and Aspen Plus backup files are given in the supplemental material. The FT liquids and surplus electricity are considered the products of the biorefinery. Various scenarios are considered and the output lower heating value (LHV) energy is compared. The energy efficiency is calculated as follows:

Energy Efficiency%
$$= (LHV \text{ of } FT \text{ liquids } [MW_{th}] + LHV \text{ of } H_2[MW_{th}] + Net \text{ Electricity } [MW_e])$$

$$/(LHV \text{ of } Biomass \text{ Feedstock } [MW_{th}]) \times 100\%$$
(10)

The LHV of materials were taken from the LCA database GREET [40]. The woody biomass was considered to have a LHV of 18 MJ/kg, the syngas was calculated to have a LHV of 8.2 MJ/kg, and the hydrogen was assumed to have a LHV of 120.1 MJ/kg. The FT liquids are the considered the FT products with a carbon chain of 5 or longer. The net electricity is the total electricity produced at the steam turbine minus the

electricity required to operate the biorefinery, especially the ASU and the AGR. The ASU was generally assumed to require a fixed 3.8% of the thermal capacity (15.2 MW) and the AGR unit was assumed to 3.5% of the plants thermal capacity (14 MW) [54]. Configurations that did not use oxygen in the ATR (the hydrogen configurations used steam) used half this percent for the oxygen required for gasification (FT-OT-E, E-25, E-40, H-E, H), and once-through configurations that required less gas cleanup beforehand, used have of this percent for the AGR (FT-OT-E, E-25, E-40). The kinetics for the various reactors are given in Table 4.

#### Economic model

The total capital investment (TCI) and production cost in gallon of gasoline equivalent (GGE) were calculated for various process configurations. We also calculated the production cost in G and in reference units to compare with current market prices. The reference units are G Diesel, G HG, and G KWh. The TCI is calculated according to the factored estimation method [66]. In this method, the cost of major plant components for a known size is obtained and a scaling factor is applied to account for the size correction for the desired equipment size according to the formula:

$$Cost_2 = Cost_1 \left(\frac{Size_2}{Size_1}\right)^{Factor} \tag{11}$$

The cost estimates in Table 7 used as the reference size and price were taken from literature [2,17,18]. A conversion factor of 1.136 was used to convert 2002 EUR to 2002 USD, specifically in reference [18]. The cost estimates used are assumed the final installed costs calculated, including the balance of plant (BOP) costs (that is installation costs such as piping, insulation, electrical connections, controls, etc.) and indirect costs (engineering, startup, insurance, contingencies, etc.) according to the methods given in the literature [2,17,18]. We used the number in Table 7 as fractions of the Total Capital Investment (TCI) and we assumed a Lang factor of 2. The Chemical Engineering Plant Cost Index (CEPCI) [67] was used to convert from the reference year dollars to the 2021 dollars. The CEPCI for years 2002, 2004, 2006, and Mar 2021 are 395.6, 444.2, 499.6, 655.9 respectively [68]. (See Table 8.).

The costs of Fischer-Tropsch liquids (FTL) production are calculated based on the method given in the EPRI technical assessment guide (TAG) report [69]. Similar equations are used for the production cost of hydrogen and electricity:

**Table 5**Biorefinery Inflows and Outflows for Various Configurations.

Configurations	Unit	FT-E	FT-E-24	FT-OT-E	FT	H2	Н2-Е	E-25	E-40
Inflow									
Air	kg/s	28.049	28.049	60.115	28.049	28.049	28.049	72.126	72.126
Water	kg/s	62.87	59.67	86.28	62.87	252.36	252.36	50.00	50.00
$O_2$	kg/s	5.33	5.33	0.00	5.33	0.00	0.00	0.00	0.00
Syngas	kg/s	32.53	32.53	32.53	32.53	32.53	32.53	32.53	32.53
Total Mass Flow	kg/s	128.79	125.58	178.92	128.79	312.94	312.94	154.66	154.66
Syngas Energy	MW	266.77	266.77	266.77	266.77	266.77	266.77	266.77	266.77
Outflow									
$CO_2$	kg/s	22.01	25.28	29.52	22.01	33.16	33.16	32.37	32.37
H <sub>2</sub> O	kg/s	75.07	73.40	101.99	75.07	249.39	249.39	66.45	66.45
$N_2$	kg/s	28.05	24.32	46.20	28.05	28.05	28.05	55.33	55.33
FT Diesel / H <sub>2</sub>	kg/s	3.657	2.596	1.214	3.657	2.287	2.287	_	_
Total	kg/s	128.79	125.59	178.92	128.79	312.89	312.89	154.15	154.15
Power	MW	36.07	54.79	83.42	0.00	6.41	0.00	118.48	160.00
Duty	MW	31.59	31.09	15.40	31.59	23.81	23.81	14.60	14.60
Net Power	MW	4.486	23.705	68.016	-31.587	-17.399	-23.814	103.876	145.400
Total Energy Output	MW	162.63	135.99	120.53	126.56	257.20	250.78	103.88	145.40
Biorefinery Efficiency		60.96%	50.98%	45.18%	47.44%	96.41%	94.01%	38.94%	54.50%
Overall Efficiency		40.66%	34.00%	30.13%	31.64%	64.30%	62.70%	25.97%	36.35%

**Table 6**Biorefinery Configurations and Notation.

Name	Description
FT-E	FT diesel is the main output. 0% of offgas is sent to the power station and 100% of offgas is recycled in the autothermal reformer (ATR)
FT	Produces FT diesel the same as FT-E, but with no power station
FT-E-24	Produces FT diesel, but 24% of offgas is sent to the power station instead of recycling in the ATR.
FT-OT-E	Produces FT diesel with no ATR and with no recycle. This is a once-through (OT) system and all offgas is sent to the power station.
H2-E	Hydrogen is the main product. Includes a power station to reclaim waste heat.
H2	Produces hydrogen the same as H2-E, but with no power station.
E-25	Electricity is the main product. All syngas is sent to the power station. This model was about 25–26% efficient.
E-40	This is a hypothetical configuration assuming 40% efficiency [75]. Assumed to have the same process emissions as E-25, but with 40% energy efficiency converting the biomass into electricity.

**Table 7**Economic parameters and calculations for the overall production costs of FT diesel for the FT-E configuration.

Parameter Value		Unit	Source
LACCR	15.41%	%/yr	[2]
Biomass cost	\$5	\$/GJ, HHV	[2]
Biomass feed	400	MW LHV	Design
O&M costs	4%	of TCI	[2]
Electricity sales price	6.65	¢/kWh	[77]
Total Capital Costs	\$ 453.744	MUS\$	Calculated
Electricity generation	4.486	MW	Aspen Simulation
FTL Production	468.5	m <sup>3</sup> /day	Aspen Simulation
FTL Prod. Cost	\$ 24.304	\$/GJ	Calculated
FTL Prod. Cost	\$ 3.171	\$/gal FT Diesel	Calculated
FTL Prod. Cost	\$ 2.746	\$/GGE	Calculated
US Avg. Gasoline Price	\$ 3.136	\$/gal Gasoline	[78]
US Avg. Diesel Price	\$ 3.342	\$/gal Diesel	[78]

software from Sphera. Fig. 3 shows the flowsheet for the LCA model in GaBi. The flows for each process are taken out of Aspen Plus and put into GaBi as new database processes. The biomass gasification object and the biorefinery were added as separate database objects. The gasification object remained the same for all configurations with the flows specified previously in Table 1. The flows for the biorefinery object changed for each configuration and are presented in Table 5.

The biomass source was specified in GaBi as wood pulp chips. The biomass is transported on a heavy-duty diesel truck for an assumed 100 miles, which is the default in GaBi and agrees with the GREET database [40] and literature [71]. All used water is assumed to be desalinated process water from a well. The oxygen used is from cryogenic oxygen separation. We assumed that this was done onsite so there is no transportation cost. Ash that is generated in the gasifier is assumed to be landfilled as inert matter. However, ash is usually stored on site in practice. Furthermore, ash can actually be mixed with soil or entrained in concrete as a filler. The electricity, if used, came from the US grid mix. If excess electricity was generated, the electricity was fed back to the

$$= \frac{[(LACCR \times TCI) + (O\&M\ Costs) + (Feedstock\ Cost \times Feedrate) - (Electricity\ Sale\ Price \times Net\ Electricity\ Production)]\ [\$/yr]}{(FT\ Liquids\ Production)\ [GJ/yr]}$$

$$(12)$$

H<sub>2</sub> Production Cost [\$/GJ]

$$= \frac{[(LACCR \times TCI) + (O\&M\ Costs) + (Feedstock\ Cost \times Feedrate) - (Electricity\ Sale\ Price \times Net\ Electricity\ Production)]\ [\$/yr]}{(H_2\ Production)\ [GJ/yr]}$$
(13)

Electricity Production Cost [\$/GJ]

$$= \frac{\left[ (LACCR \times TCI) + (O\&M\ Costs) + (Feedstock\ Cost \times Feedrate) \right] \left[ \$/yr \right]}{(Net\ Electricity\ Production)\ [GJ/yr]}$$
(14)

where LACCR is the levelized annual capital charge rate defined as the annual percentage of the total capital investment (TCI) charged as portion of the energy products sold each year. The LACCR was calculated to be 15.41%/yr based on the work by Kreutz et al. [2] assuming an annual interest rate of 7% a construction period of 3 years and a plant lifetime of 20 years. Parameters for the FTL production cost equation are listed in Table 7. The operation and maintenance (O&M) costs were not calculated in detail and were simply assumed to be 4% of the TCI as done in literature [2]. This method was also used for technoeconomic analysis (TEA) of similar coal-to-liquids (CTL) plants and was used for other TEA of gasification facilities by NETL [70]. The biomass was purchased at an assumed rate of \$5/GJ HHV or \$4.587/GJ LHV.

Life cycle assessment model

The life cycle assessment (LCA) model was performed in GaBi, a LCA

grid and offset the US grid mix. This was simulated as a negative flow back to the grid (positive being consumption). This applies a carbon offset to the LCA, because this electricity is being fed back to the grid and offsets electricity that would have been made from mixed sources of mostly fossil fuels, but also nuclear and other renewables. This mix of electricity sources in GaBi is considered to emit an average of 0.511 kg CO<sub>2</sub>/kWh which agrees with the U.S. Energy Information Administration (EIA) and the U.S. Environmental Protection Agency (EPA) which estimate about 0.463 kg CO<sub>2</sub>/kWh [72-74], and considers distribution and other losses. Both the product FT diesel and hydrogen are considered to travel 100 miles in a heavy duty tank truck before reaching the filling station. Carbon emissions at the filling station where not considered in this LCA because of a lack of data and because the environmental impact of the storage is considered negligible compared to the other processes. Finally, each fuel stream produced is used in a car. The FT diesel is used in a 2019 Chevy Cruise 1.6 L, 4 cylinder, automatic

**Table 8**Factored Cost Estimation Method for TCI using Major Equipment for FT-E Plant Configuration.

	Base Cost (MUS\$)	Base Capacity	Base Unit	Scale Factor	Base Year	Desired Capacity	Factored TPI (Base Year)	CEPCI Factor	Factored TCI	Ref.
Unit										
Air separation unit	23	24	tonne O <sub>2</sub> /h	0.75	2002	43.2	35.742	1.658	59.260	[17]
Pretreatment and gasification										
Conveyers	0.33	69.54	MWth LHV	0.8	2002	400	1.338	1.658	2.218	[17]
Grinding	0.43	69.54	MWth LHV	0.6	2002	400	1.228	1.658	2.037	[17]
Storage	1.05	69.54	MWth LHV	0.65	2002	400	3.274	1.658	5.428	[17]
Dryer	7.71	69.54	MWth LHV	0.8	2002	400	31.255	1.658	51.820	[17]
Iron removal	0.33	69.54	MWth LHV	0.7	2002	400	1.123	1.658	1.862	[17]
Feeding system	0.38	69.54	MWth LHV	1	2002	400	2.186	1.658	3.624	[17]
IGT gasifier	30	367	MWth LHV	0.7	2002	400	31.864	1.658	52.830	[17]
Gas cleaning			LH1 V							
Cyclone	2.57	69.54	MWth LHV	0.7	2002	400	8.746	1.658	14.501	[17]
Syngas Cooling	2.95	69.54	MWth LHV	0.7	2002	400	10.039	1.658	16.645	[17]
Particulate Filter	1.62	69.54	MWth LHV	0.65	2002	400	5.051	1.658	8.375	[17]
Condensing Scrubbers	2.57	69.54	MWth LHV	0.7	2002	400	8.746	1.658	14.501	[17]
Hot Gas Cleaning (Rectisol)	14.3	367	MWth LHV	0.7	2002	400	15.188	1.658	25.182	[17]
Guard beds (ZnO & active C)	0.027	8	Nm3 gas/ s	1	2002	32.82	0.112	1.658	0.1854	[18]
Syngas processing Recycle compressor	1.617	2	MWe	0.67	2007	1.745	1.475	1.248	1.842	[2]
ATR reactor	30.3	400	MWth LHV	0.7	2007	400	30.3	1.658	50.237	[17]
WGS reactor	0.45	2400	kmol/h	0.6	2002	5271	0.721	1.658	1.196	[17]
PSA unit A + B FT production and upgrading	32.6	9600	kmol/h	0.7	2002	5271	21.427	1.658	35.525	[18]
FT feed compressor	1.617	2	MWe	0.67	2007	0.141	0.273	1.248	0.341	[2]
FT reactor	1.880	66,978	Nm3/h	0.75	2007	118,144	2.877	1.248	3.592	[2]
FT product upgrading	264.8	286	m3 FTL/ h	0.7	2002	13.86	31.819	1.248	52.755	[18]
Power production										[18]
Gas Turbine	22	26.3	MWe	0.7	2002	12	12.702	1.658	21.060	[18]
Steam Turbine + System Expansion Turbine Total Capital	5.9 5	10.3 10.3	MWe MWe	0.7 0.7	2002 2002	18.3 22	8.822 8.505	1.658 1.658	14.627 14.101 <b>453.744</b>	[18] [18]

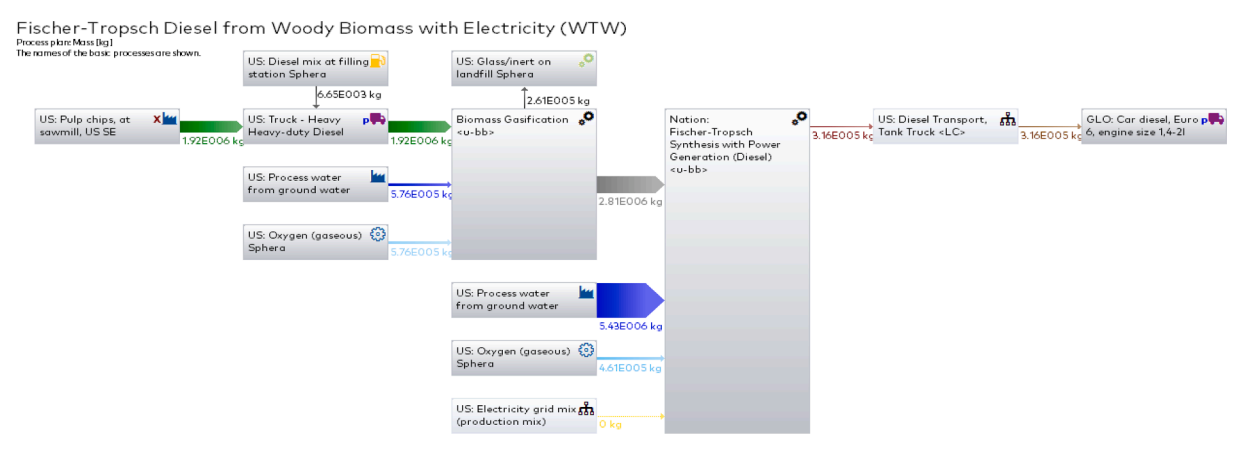


Fig. 3. Life Cycle Assessment (LCA) model in GaBi outflows for Fischer-Tropsch diesel and electricity production.

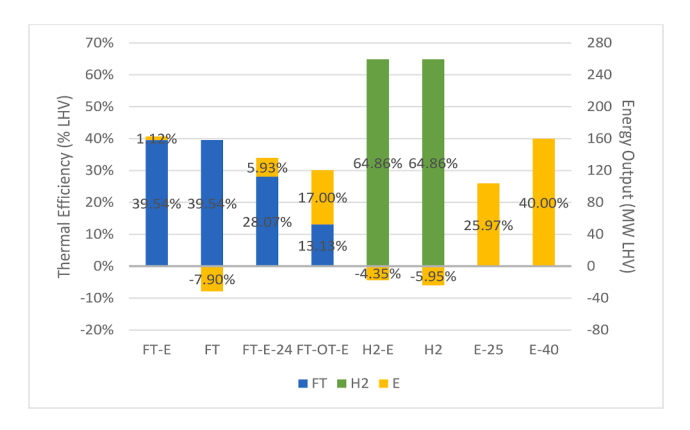
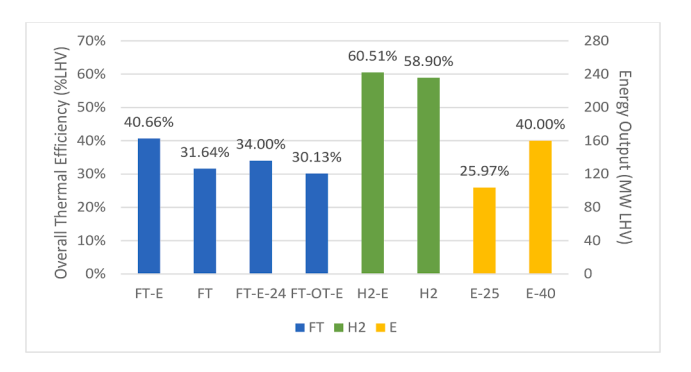


Fig. 4. Thermal efficiency for different biorefinery configurations comparing the energy produced and consumed in various forms: FT liquids,  $H_2$ , and Electricity.



**Fig. 5.** Net thermal efficiency and combined energy output for Fischer-Tropsch (FT), Hydrogen (H2), Electricity (E) biorefinery configurations.

9-speed turbo diesel with a fuel economy of 37 miles per gallon. In GaBi, the emissions are modeled as a Euro 6 1.4-2L diesel car. The hydrogen is used in a 2021 Honda Clarity fuel cell vehicle with a fuel economy of 67 miles/kg H<sub>2</sub>. The electricity is used in a 2021 Tesla Model S Long Range Automatic (A1) with an economy of 3.57 miles/kWh. The hydrogen and electric vehicles were assumed to have no emissions (i.e., the oxygen consumption and water exhaust of the hydrogen vehicle were not considered in the LCA). Any emissions from the construction costs of the

biorefinery equipment or the cars were not considered in this LCA. The LCA software GaBi is able to consider many different environmental outcomes of the process, such as human toxicity, acidification, water ecotoxicity, and land use changes, but the only environmental outcome considered in this study was the greenhouse gas emissions as kg of  $\rm CO_2$  equivalent.

### Results and discussion

Many configurations for the biorefinery were considered. The three main products are FT diesel, hydrogen, and electricity. However, with FT diesel production and hydrogen production, electricity can be generated from waste heat, but this requires a higher capital cost to build the power station. Also, when producing FT diesel, recycling the off-gas and using an autothermal reforming (ATR) can increase FT diesel yield, but again, there is higher capital cost to build the ATR unit. The specific biorefinery configurations considered in this study and the notation for each are given in Table 6.

## Process efficiency

The biorefinery efficiency is given in Fig. 4 and Fig. 5 for the configurations studied. This is calculated as the energy value of the products minus the electricity used divided by the energy value of the input biomass fuel. The percent of energy produced and used in different forms is shown in Fig. 4, specifically if net electricity is used it is shown as a negative efficiency, but if net electricity is produced it is shown as a positive efficiency. In Fig. 5, only the overall net thermal efficiency is given.

For the FT-E and FT configurations, 39.5% of the input biomass energy (LHV basis) was converted to FTL. The overall thermal efficiency for FT-E was 40.7% including the electricity generation from the burned offgas, which is similar to values reported in other studies [17–19]. The FT configuration which did not have a power station consumed electricity and had a net efficiency of 31.6%. Similarly, the power station improves efficiency for hydrogen production as well, as seen with the H2 configuration being 58.9% efficient while H2-E is 60.5% efficient. This minor improvement in efficiency would need to be justified by a reduction in production cost, which is seen later in Section 3.2. Finally, the E-25 configuration, which produces only electricity, does not need extensive gas cleanup, water–gas shift, an FT unit, or an AFR unit. It is only about 26% efficient in our simulation, because our biorefinery was not optimized for electricity production and only uses a single steam cycle. In practice, between 35% and 45% efficiency for electricity

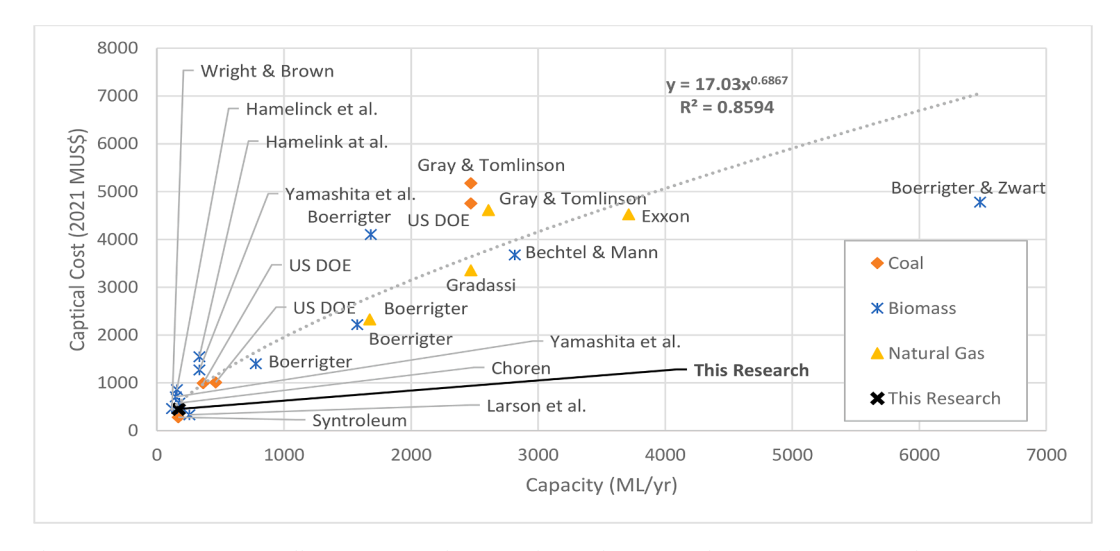
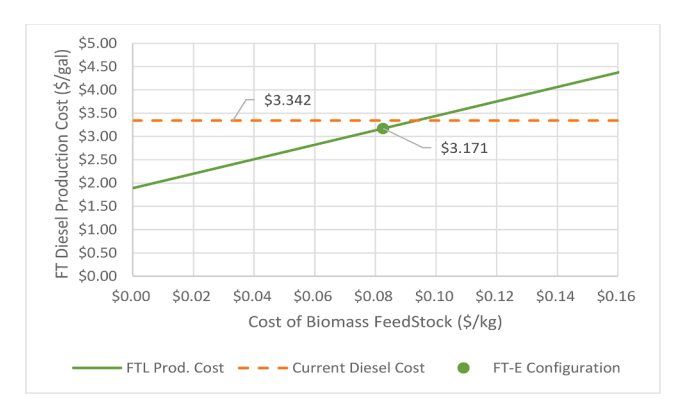


Fig. 6. Total Capital Investment (in Mar 2021 million USD) vs Fischer-Tropsch Liquids (FTL) Production Capacity for Coal, Biomass, and Natural Gas Plants (data from Searcy et al. [76]).



**Fig. 7.** Cost of FTL Production Cost vs. Cost of Biomass Feedstock with Current Diesel Price shown for comparison, and this current FT-E configuration with the assumed \$5/MJ HHV of Biomass.



**Fig. 8.** Capital cost of biorefinery configurations (FT: Fischer-Tropsch, H2: Hydrogen, E: Electricity, for notation see Table 6).

production can be achieved with an integrated gasification combined cycle (IGCC) plant with both a gas cycle and a steam cycle. Therefore, we included a hypothetical configuration E-40 that produced electricity at 40% efficiency to see if this would make electricity from biomass attractive. This biorefinery model can be considered a conservative estimate for electricity production.

The gaseous portion of FT synthesis product contains gaseous light hydrocarbons  $C_1$ - $C_4$ ,  $CO_2$  (in iron FT synthesis), and small amounts of  $H_2$  and CO. This offgas can be either burned in a boiler or gas turbine to generate electricity or reformed to produce additional syngas to recycle back into the FT reactor. The addition of an autothermal reformer (ATR)

can carry significant capital and operating costs that must be justified [17,18]. The use of an ATR helps recover some carbon that would otherwise be lost and use it to create more FT hydrocarbons. This can be seen in Fig. 5 by comparing configurations FT-E and FT-OT-E. The oncethrough (OT) design does not have an ATR or recycle loop and it is less efficient. The total energy conversion efficiency improves by about 33% for the biorefinery when FT liquids were the main product (as opposed to electricity) by adding the ATR and recycle loop. When the offgas is burned to produce electricity (instead of reformed and recycled) electricity is more of a co-product than a byproduct. However, using offgas for electricity for co-generation slightly decreases the overall energy efficiency because converting syngas to FT liquids is more efficient than conversion to electricity in a steam or gas turbine in this facility. The FT-E-24 configuration recycles 24% of the off-gas to the ATR unit was included because this was previous studied [35] and it provides a midpoint between the FT-OT-E and the FT-E configurations.

#### Economic analysis

The production costs of FT diesel, hydrogen, and electricity were calculated for the different biorefinery configurations given in Table 6. The total capital costs and production costs of FT biofuels were calculated using the methods discussed in Section 2.2 and are shown in Fig. 8 and Fig. 9 and given in Table 9. The ATR recycle designs give lower costs of FT biofuels than the OT design, even though it requires 6 to 9% higher capital cost for the ATR unit, mainly because the biorefinery is able to more efficiently convert the biomass into FT liquid with the recycle loop. Some other studies in literature show the opposite, that the ATR unit would not decrease the cost of FT fuels [17,18]. Our study shows the ATR lowers production cost because we have configured the biorefinery to maximize the production of FT liquids and minimize the excess electricity production, while the other studies mentioned previously attempt to balance co-generation of FT liquids and electricity.

The capital costs shown in Fig. 8 were compared against data from Searcy et al. [76] which is shown in Fig. 6. This data gives the following equation for calculating capital cost in 2021 million USD:

Capital Cost [MUSD] = 
$$17.03*(FTL\ Production\ Capacity[ML/year])^{0.6867}$$
 (15)

Using Equation (15), the capital cost for the FT-E configuration which produces 171.1 million L [ML]/year is estimated to be \$581.9 million USD. Our calculated TCI was \$452.7 MUSD, which is within the 30% variance when using factored and empirical cost estimation methods [66].



Fig. 9. Production cost compared to reference market price for different biorefinery configurations [77,78].

**Table 9**Production Values for the Different Biorefinery Configurations.

Configurations	FT-E	FT	FT-E-24 <sup>a</sup>	FT-OT-E	Н2-Е	H2	E-25	E-40 <sup>b</sup>
Production	315.9	315.9	224.3	104.9	197.6	197.6	2493.0	3840.0
Production Unit	kg FTL/day	kg FTL/day	kg FTL/day	kg FTL/day	tonne H <sub>2</sub> /day	tonne H <sub>2</sub> /day	MWh/day	MWh/day
TCI (MUS\$)	\$453.74	\$403.96	\$453.74	\$401.67	\$353.89	\$347.27	\$327.14	\$327.14
Production Costs (\$/GJ)	\$24.304	\$26.230	\$31.554	\$49.119	\$15.779	\$16.062	\$37.034	\$24.044
Production Cost (\$/GGE)	\$2.746	\$2.963	\$3.565	\$6.409	\$1.860	\$1.893	\$4.301	\$2.792
Production Cost	\$3.171	\$3.422	\$4.117	\$6.409	\$1.895	\$1.929	\$13.332	\$8.656
Refence Unit	\$/gal Diesel	\$/gal Diesel	\$/gal Diesel	\$/gal Diesel	\$/kg H <sub>2</sub>	\$/kg H <sub>2</sub>	¢/kWh	¢/kWh
Efficiency	0.4066	0.3164	0.2017	0.3013	0.6051	0.5890	0.2597	0.4000
FT (MW) <sup>c</sup>	158.14	158.14	112.29	52.52	_	-	-	-
H <sub>2</sub> (MW)	-	_	-	-	259.43	259.43	-	-
E (MW)	4.49	-31.59	-31.59	68.02	-17.40	-23.81	103.88	160.00
tonne CO <sub>2</sub> / day GTG <sup>d</sup>	1902	1902	2184	2550	2865	2865	2797	2797
tonne CO <sub>2</sub> / day WTW	3120	3750	2890	2350	3350	3430	3040	3040
tonne CO <sub>2</sub> [+biogenic] / day WTW <sup>e</sup>	-395	47.7	-645	-1210	-217	-138	-525	-526
M miles / day	3.875	3.875	2.751	1.287	12.506	12.506	8.904	13.714
miles / kg Biomass	2.018	2.018	1.433	0.670	6.513	6.513	4.637	7.143
kg CO <sub>2</sub> / mile [GTG]	0.491	0.491	0.564	0.658	0.739	0.739	0.722	0.722
kg CO <sub>2</sub> / mile [WTW]	1.546	1.858	1.432	1.165	1.660	1.700	1.506	1.506
kg CO <sub>2</sub> / mile [WTW + biogenic]	-0.805	0.097	-1.314	-2.465	-0.442	-0.281	-1.070	-1.072
Reference Price	\$3.342	\$3.342	\$3.342	\$3.342	\$3.00	\$3.00	\$0.0665	\$0.0665
Reference Unit	\$/gal Diesel	\$/gal Diesel	\$/gal Diesel	\$/gal Diesel	\$/kg H <sub>2</sub> <sup>f</sup>	\$/kg H <sub>2</sub> <sup>f</sup>	\$/kWh	\$/kWh
Reference Price (\$/GJ)	\$25.61	\$25.61	\$25.61	\$25.61	\$24.98	\$24.98	\$18.47	\$18.47
Profit \$/GJ	\$1.31	-\$0.62	-\$5.94	-\$23.51	\$9.20	\$8.92	-\$18.56	-\$5.57
kg CO <sub>2</sub> /GJ	-0.0589	0.0071	-0.1355	-0.5434	-0.0197	-0.0125	-0.1192	-0.0775
Profit \$/kg CO <sub>2</sub> seq.	\$22.24	-\$86.71	-\$43.85	-\$43.26	\$466.52	\$711.01	-\$155.73	-\$71.86
kg CO <sub>2</sub> seq. / \$ Profit	0.044971	-0.01153	-0.02281	-0.02312	0.002144	0.001406	-0.00642	-0.01392

<sup>&</sup>lt;sup>a</sup> The FT-E-24 configuration split 24% of the offgas to send to the power station, the remaining 76% went to be reformed and recycled.

<sup>&</sup>lt;sup>e</sup> The Gate-to-Gate amount does not include an offset for electricity generated and does not include biogenic CO<sub>2</sub> absorption or emission, the WTP and WTW include the offset for electricity and biogenic CO<sub>2</sub> absorption.



Fig. 10. Production costs for different types of hydrogen [22,25].

biorefinery configurations. Fig. 5 shows the thermal energy efficiency and combined energy output as calculated by Equation (10). The hydrogen configurations were the most efficient group with H2-E being the most efficient configuration combining hydrogen production and electricity production from waste heat recovery, mostly from the syngas. The FT-E configuration was the most efficient of the FT synthesis options, combining electricity production from waste heat recovery but recycling offgas 100% (i.e., no offgas was sent to the power station, the electricity was generated solely from waste heat from gasification and the FT reactor, and all offgas is recycled to the ATR). The E-25 option generated electricity at about 26%. This is the configuration that was modeled in Aspen Plus with no ATR and all syngas being combusted in the power station. The E-40 was a hypothetic configuration which was not modeled in Aspen. This was assuming the biorefinery was able to reach an energy efficiency of 40% as reported in literature [75]. Fig. 7 shows the effect of the biomass feedstock price on the production price.

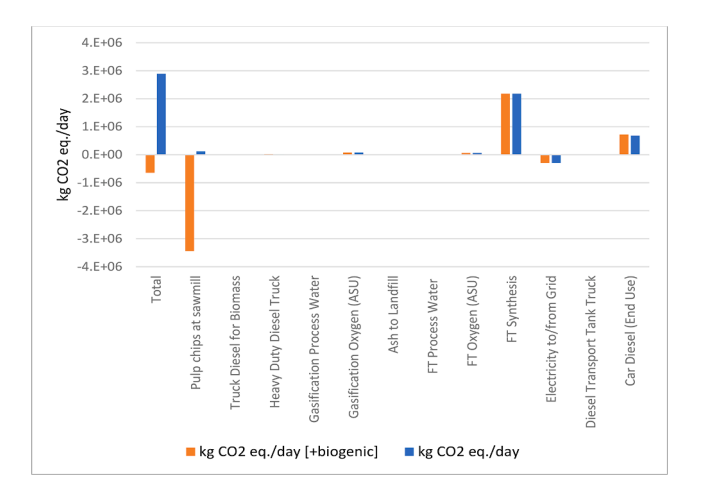


**Fig. 11.** GHG emissions from each stage in the life cycle of the biomass from cradle-to-grave (CTG) for FT-E-24 configuration.

The profitability of the ATR can be increased by maximizing the recycle ratio and thus the yield of FT liquids. This is shown in Fig. 5 by comparing the FT-OT-E and the FT-E cases. The efficiency of the iron FT process is increased with the addition of an ATR because the iron FT catalyst produces a large volume of offgas ( $C_1$ -C4- hydrocarbons and  $CO_2$ ). It is also interesting to note that although reducing the  $CO_2$  removal in the AGR reactor increased the volume of syngas, it also increased the yield of FT liquids. Comparing the capital costs and production costs in Fig. 8 and Fig. 9 and Table 9 shows that the increased costs due to larger gas volumes were offset by the increased yield of FT liquids and reduced effort of  $CO_2$  removal. Requiring less  $CO_2$  removal means that cheaper and less energy intensive  $CO_2$  removal processes can

b This configuration was not one that we built, but we assumed the electricity production efficiency based on [79].

<sup>&</sup>lt;sup>c</sup> All energy values are given based on the Lower Heating Value (LHV).

 $<sup>^{</sup>m d}$  Gate-to-Gate (GTG) accounts for the CO $_2$  emissions in the biorefinery, Well-to-Pump (WTP) or Cradle-to-Gate accounts for production emissions from resources as well, Well-to-Wheel (WTW) or Cradle-to-Grave (CTG) accounts for CO $_2$  emissions over the life cycle of the biomass.

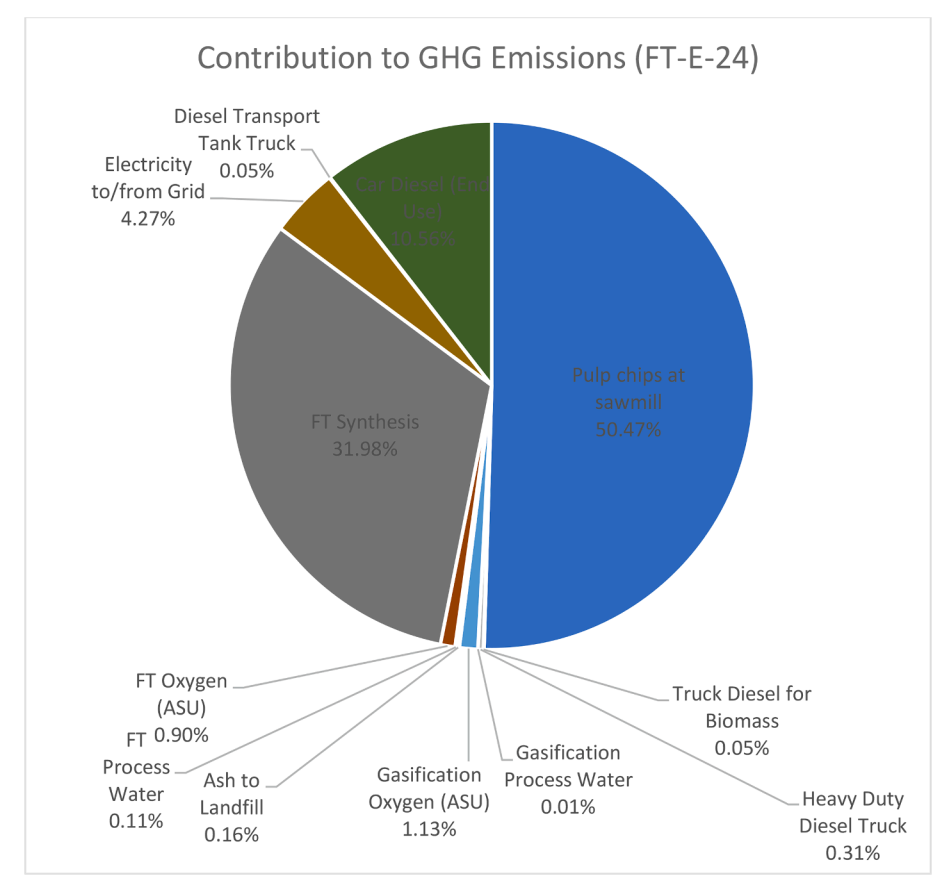


Fig. 12. Absolute magnitude of GHG contributions to the overall GHG emissions.

be used such as membrane and adsorption based processes, which would give further cost advantages to the iron FT process that are not considered here.

Fig. 9 shows the FT diesel, hydrogen, and electricity production costs for different configurations compared to a reference price. The reference prices were taken from what was considered an averages sales price for each type of fuel. The FT diesel was compared to the nationwide average sale price for diesel [78]. The electricity reference price was the national average sales price for commercial electricity [77]. Finally, the prices for hydrogen are greatly varied. Fig. 10 shows the price of hydrogen based on fuel source. A reference price of \$3/kg was chosen for hydrogen. This is very low for green hydrogen and very high for fossil fuel sources, but it is far below what would be paid at the pump for a hydrogen fueled vehicle [22,25].

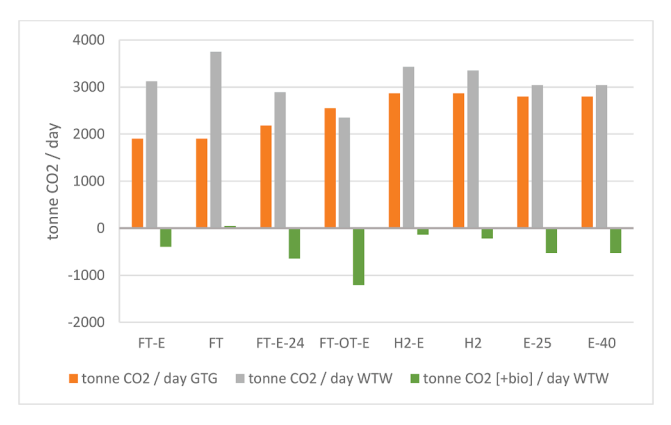


Fig. 13. GHG emissions for each biorefinery configuration.

Environmental analysis and life cycle assessment (LCA)

The LCA in GaBi shows which processes in the biorefinery contributed the most to the overall GHG emissions. The LCA model is described in Section 2.3 and illustrated in Fig. 3. The results given in Fig. 11 show the GHG emissions in kg CO<sub>2</sub> equivalent at each stage in the life cycle of the biomass from cradle-to-grave (CTG)—or well-to-wheel (WTW) as it is called with transportation fuels—for the FT-E-24 configuration. The first measure includes fossil and biogenic GHG emissions and absorptions. The second measure is only process emissions. The total carbon emissions (including biogenic sinks) are negative. This is because the wood biomass absorbed more carbon in its lifetime as a tree than is emitted in the biorefinery or in using the fuel in a vehicle. This is aided mainly by two things: (1) some of the carbon is being sequestered again as ash and unconverted char, (2) electricity is produced as a co-product and offsets CO<sub>2</sub> emissions from electricity generated from other fossil fuels. The second point is seen as the negative value in Fig. 11 at the item labeled "Electricity to/from Grid". The first point is not shown as a negative emission, but as less GHG emissions in the biorefinery than could have been released. The ash and unconverted char actually represent a process inefficiency. If the biomass gasifier is more efficient at converting the carbon into syngas, then less carbon is sequestered in the ground. A coal gasifier could also do this by not converting as much of the carbon to syngas, but coal is considered a non-renewable resource and it would take millions of years to reform the coal again. But with biomass and sustainable farming, we can continue to sustainably harvest the biomass and sequester some of the carbon as ash and char and have a carbon negative process over the life-cycle of the biomass.

Fig. 12 shows the absolute magnitude of each process' GHG emissions (including biogenic emissions) for the FT-E-24 configuration. The pie chart represents the percent contribution that each process has to the overall GHG emission of the life cycle. This shows us that the biggest

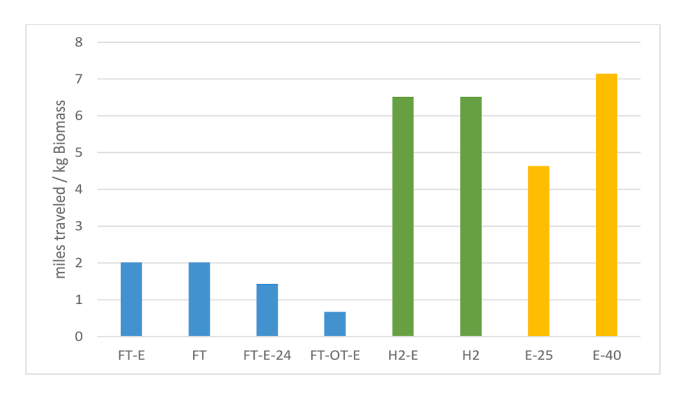


Fig. 14. Miles traveled per kilogram of biomass for different biorefinery configurations.

contributors to the overall GHG emissions are in order of magnitude: (1) the  $\mathrm{CO}_2$  absorbed by the biomass, (2)  $\mathrm{CO}_2$  emitted by the biorefinery (mostly in the AGR and power station exhaust), (3) the combustion of the FT diesel in a vehicle, and (4) the offset from electricity coproduction. All the other process are at least one order of magnitude smaller in GHG emissions, but the next largest GHG emitter is the oxygen separation units.

Fig. 13 shows the GHG emissions for each of the different biorefinery configurations in three different categories: (1) gate-to-gate (GTG) emissions, meaning only emissions from the gasifier and biorefinery, (2) well-to-wheel (WTW) emissions excluding biogenic absorptions and emissions, and (3) WTW emissions including biogenic emissions. Configuration FT-OT-E which produces FT diesel in a once-through system shows the most carbon sequestered (the least/most negative carbon emissions). The FT-OT-E co-produces the most electricity of the FT configurations and therefore has a larger offset. The FT configuration which has no power station uses electricity from the grid, especially for the ASU and AGR. This configuration has the highest WTW carbon emissions, and it was the only configuration out of those considered that had net positive carbon emissions.

Comparison of biorefinery product configurations for multiple objectives

## Miles per kilogram biomass

There are many different objectives one could consider when deciding which biorefinery configuration to build. The two most obvious objectives are profitability and GHG emissions. GaBi has many other environmental objectives calculated in the LCA that were not considered in this research, such as human toxicity, acidification, water and soil ecotoxicity, land use changes, and many more. However, one that is not often considered is miles per kg of fuel. Using the passenger car models discussed in Section 2.3, we calculated the miles per kg of biomass using the Aspen Model and efficiencies calculated for the configurations in

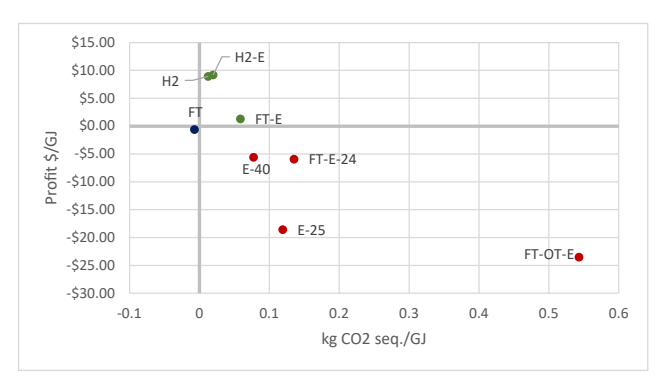


Fig. 15. Comparing profit to CO<sub>2</sub> sequestered.

Table 6. Again, the FT diesel is used in a 2019 Chevy Cruise 1.6 L, 4 cylinder, automatic 9-speed turbo diesel with a fuel economy of 37 miles per gallon, the hydrogen is used in a 2021 Honda Clarity fuel cell vehicle with a fuel economy of 67 miles/kg  $\rm H_2$ , the electricity is used in a 2021 Tesla Model S Long Range Automatic (A1) with an economy of 3.57 miles/kWh. This is displayed in Fig. 14. Each of these configurations that produced electricity was assumed to feed the electricity back to the grid for general use, they were not assumed to use the electricity for electric vehicles. The figure shows that the hypothetical scenario of producing electricity at 40% efficiency yields more miles per kg biomass than the other configurations, and hydrogen production with fuel cell vehicles being the second best.

#### Comparing CO2 sequestered and profit

Since all of the configurations except one had net negative carbon emissions over the life cycle of the biomass, we compared the kg CO<sub>2</sub> sequestered and the profit. The production costs were determined in Section 3.2 and production costs and reference market prices are listed in Table 9. Subtracting the market price from the production cost, we calculated an estimate of the profit, ignoring working capital, marketing and distribution costs, tax credits, carbon credits, or renewable energy credits (RECs). Comparing the profit in USD \$2021 per GJ to the kg CO<sub>2</sub> sequestered per GJ, we see in Fig. 15 that there are three configurations (H2-E, H2, and FT-E) that are both profitable and sequester carbon (net negative carbon emissions). One configuration (FT) that is doubly negative in that it emits carbon and is not profitable in current market conditions, but it is very close to the threshold on both fronts and perhaps small changes in market conditions or in the configuration of the biorefinery could make it profitable and/or have net negative emissions. The other FT configurations and both of the electricity configurations considered were not profitable but did sequester carbon. Because the E-40 and FT-E-25 configurations were also close to the threshold of profitability, it could be that with enough credits from other markets (tax, carbon, RECs, etc.) or changes in the biorefinery configuration these options could be made profitable. These figures show that the hydrogen configurations are the most profitable, but sequester less carbon, and the FT-E configuration is less profitable but sequesters more carbon.

#### Conclusions

This study preformed Aspen Plus and GaBi LCA simulations of a biomass biorefinery with three main product streams: Fischer-Tropsch (FT) synthesis for synthetic diesel, hydrogen production, and electricity. All of these products were considered for use in passenger cars. The biorefinery model considered water-gas shift (WGS) and acid-gas removal (AGR) reactors and an autothermal reforming (ATR) unit. The process simulation was kinetics based and the reaction kinetics and reactor sizes are given in Table 4. The overall thermal efficiency as defined by Equation (10) and can be seen for various process configurations in Fig. 5. For the biomass-to-liquids (BTL) configurations, the efficiency ranged from 20-41%. For the biomass-to-hydrogen (BTH), the efficiency was between 58 and 61%. For electricity production, the biorefinery was only 26% efficient. Including an ATR reactor for reforming the offgas and recycling it back into the FT reactor greatly improves the FT production economics and the overall thermal efficiency, as seen by comparing the FT-E and the FT-OT-E configurations, because converting biomass to FT liquids is more energy efficient than converting to electricity. The biorefinery can even more efficiently convert biomass to hydrogen. The capital costs for different biorefinery configurations ranged from \$327-454 million USD and are given in Table 7 and shown in Fig. 8. For FT diesel configurations, the production costs ranged from 3.171 to 6.409 \$/gal, for hydrogen, production costs were 1.895-1.929 \$/kg H2, and for electricity production cost was 0.133 \$/kWh and can be seen compared to reference market prices in Fig. 9. The H2-E configuration was found to be the most profitable. The

LCA showed the gate-to-gate and well-to-wheel GHG emissions by using this biorefinery's products in modern passenger vehicles. Including biogenic carbon absorption and emissions, all but one configuration had net negative carbon emissions. The FT-OT-E configuration had the most negative carbon emissions but was also the least profitable. The FT-E configuration had the most negative GHG emissions while still being positive. Fig. 15 compares the profit and carbon emissions. When considering transportation miles, Fig. 14 shows the miles per kg biomass with the E-40 configuration yielding the highest miles at 7.14 miles/kg biomass and the hydrogen configurations with 6.51 miles/kg biomass. It has been shown that biomass has the potential to be net negative in carbon emissions while producing fuel for transportation. Hydrogen production seems to be the most profitable and promising, even though hydrogen fuel cell vehicles and hydrogen distribution are not as widespread. Until hydrogen distribution for fuel cell vehicles is more established, the most profitable and yet still possibly carbon negative, may be the production of ammonia, but ammonia production was not considered in this research. The production of FT diesel can also be made profitable while still achieving net negative carbon emissions.

#### Future work

Many assumptions were made in this model and there is much room for improvement. Some main areas of improvement are:

- This economic model does not consider working capital, marketing
  and distribution costs, tax credits, carbon credits, or renewable energy credits. It simply compared the production cost to the current
  market price. A more thorough analysis would reveal the effects of
  these costs on the profitability of the biorefinery.
- The thermal efficiency of this gasification model is less than the thermal efficiency found in other models and in practice [35].
   Increasing the efficiency of this process will increase the efficiency of the entire process, but could also lead to more carbon emissions if carbon from the biochar is released.
- The LHV efficiency of the power generation station in our model is between 20 and 25% because it is a single steam cycle. This is much less efficient than power stations in practice, which are combine cycle and can be around 40% efficient or more [75]. However, this work can provide a conservative estimate, since the power station is less efficient. Considering a combined cycle, more efficient power station is an area of improvement.
- The gasifier could be operated in such a way that the WGS unit and ATR unit would not be necessary. This should be tested, because previous literature has shown that separate reactors are more efficient [19].
- This study (process simulation, economic model, and LCA) made some simplifying assumptions. A more detailed model will need to be conducted to confirm the findings in this work.
- LCA considered much more than GHG emissions and carbon footprint, such as but for simplicity carbon emissions are the only metric considered here.
- Consider ammonia production in the TEA and LCA, because the largest use of syngas and hydrogen in the US is for ammonia production for fertilizer. This may be the most profitable avenue for a biorefinery.

## CRediT authorship contribution statement

Micah Jasper: Writing – original draft, Conceptualization, Methodology, Investigation. Navid Rafati: Conceptualization, Writing – review & editing. Keith Schimmel: Writing – review & editing. Abolghasem Shahbazi: Writing – review & editing. Fanxing Li: Writing – review & editing. Mark Mba-Wright: Writing – review & editing. Lijun Wang: Conceptualization, Supervision, Writing – review

& editing.

#### **Declaration of Competing Interest**

The authors declare that they have no known competing financial interests or personal relationships that could have appeared to influence the work reported in this paper.

#### Acknowledgements

This project was supported by funds provided by an National Science Foundation CREST Project (Award Numbers: 1736173 and 2112679) and contributions from NC A&T State University. Its contents are solely the responsibility of the authors and do not necessarily represent the official views of the funding agency. Mention of trade names, proprietary products, or company names is for presentation clarity and does not imply endorsement by the authors, the university, or the funding agency.

#### Appendix A. Supplementary data

Additional gasification models are described in the appendix. There are additional tables and figures. All data and code is given at this link: https://bit.ly/Jasper-2021-ECM. Supplementary data to this article can be found online at https://doi.org/10.1016/j.ecmx.2022.100208.

#### References

- Ackrill, R. Kay, A. The growth of biofuels in the 21st century: policy drivers and market challenges. 2014, Palgrave Macmillan: London. p. XVII, 250.
- [2] Kreutz TG, et al. Fischer-Tropsch Fuels from Coal and Biomass. Pittsburgh, Pennsylvania, USA: Princeton University; 2008.
- [3] Sims REH, Mabee W, Saddler JN, Taylor M. An overview of second generation biofuel technologies. Bioresour Technol 2010;101(6):1570–80.
- [4] Li G, et al. Life cycle assessment and techno-economic analysis of biomass-tohydrogen production with methane tri-reforming. Energy 2020;199:117488.
- [5] Eilers J, Posthuma SA, Sie ST. The shell middle distillate synthesis process (SMDS). Catal Lett 1990;7(1):253–69.
- [6] Goellner, J.F., et al., Analysis of Natural Gas-to Liquid Transportation Fuels via Fischer-Tropsch. 2013, National Renewable Energy Laboratory: US DOE / NETL / Office of Fossil Energy.
- [7] Espinoza RI, Steynberg AP, Jager B, Vosloo AC. Low temperature Fischer-Tropsch synthesis from a Sasol perspective. Appl Catal A 1999;186(1-2):13–26.
- [8] Steynberg AP, Nel HG. Clean coal conversion options using Fischer-Tropsch technology. Fuel 2004;83(6):765–70.
- [9] Damartzis T, Zabaniotou A. Thermochemical conversion of biomass to second generation biofuels through integrated process design—A review. Renew Sustain Energy Rev 2011;15(1):366–78.
- [10] Brown TR, Wright MM. A Framework for Defining the Economic Feasibility of Cellulosic Biofuel Pathways. Biofuels 2014;5(5):579–90.
- [11] Dutta A, Phillips SD. Thermochemical Ethanol via Direct Gasification and Mixed Alcohol Synthesis of Lignocellulosic Biomass. United States: National Renewable Energy Laboratory; 2009.
- [12] Phillips, S., et al., Thermochemical Ethanol via Indirect Gasification and Mixed Alcohol Synthesis of Lignocellulosic Biomass. 2007, National Renewable Energy Laboratory.
- [13] Phillips, S.D., et al., Gasoline from Wood via Integrated Gasification, Synthesis, and Methanol-to-Gasoline Technologies. 2011, National Renewable Energy Laboratory.
- [14] Dry ME. The Fischer-Tropsch process: 1950–2000. Catal Today 2002;71(3-4): 227–41.
- [15] Dry, M.E., Fischer-Tropsch Technology; Studies in Surface Science and Catalysis, Volume 152. 2004: Els.
- [16] Swanson, R.M., et al., Techno-Economic Analysis of Biofuels Production Based on Gasification. 2010, National Renewable Energy Lab: United States. p. Medium: ED; Size: 165 pp.
- [17] Tijmensen MJA, et al. Exploration of the possibilities for production of Fischer Tropsch liquids and power via biomass gasification. Biomass Bioenergy 2002;23 (2):129–52.
- [18] Hamelinck C, Faaij A, Denuil H, Boerrigter H. Production of FT transportation fuels from biomass; technical options, process analysis and optimisation, and development potential. Energy 2004;29(11):1743–71.
- [19] Leibbrandt NH, Aboyade AO, Knoetze JH, Görgens JF. Process efficiency of biofuel production via gasification and Fischer-Tropsch synthesis. Fuel 2013;109:484–92.
- [20] Willette, S., Don't Forget About Biomass Gasification For Hydrogen, in Forbes. 2020.
- [21] Binder, M., et al., Hydrogen from biomass gasification. 2018: IEA Bioenergy.
- [22] IEA, The Future of Hydrogen, F. Birol, Editor. 2019, International Energy Agency.
- [23] Milne, T.A., Elam, C.C., Evans R.J. Hydrogen from biomass: state of the art and research challenges; 2002: United States.

- [24] Edwardes-Evans, H. Green hydrogen costs need to fall over 50% to be viable: S&P Global Ratings. 2020 20 Nov 2020 [cited 2021 08/02/2021]; Available from: https://www.spglobal.com/platts/en/market-insights/topics/hydrogen.
- [25] Baronas, J. Achtelik, G. Joint Agency Staff Report on Assembly Bill 8: 2019 Annual Assessment of Time and Cost Needed to Attain 100 Hydrogen Refueling Stations in California. 2019, California Energy Commission.
- [26] DOE. Hydrogen Fueling Station Locations. 2021; Alternative Fuels Data Center]. Available from: https://afdc.energy.gov/fuels/hydrogen\_locations.html#/find/nearest?fuel=HY.
- [27] Ohi, J.M., Vanderborgh, N. Consultants, G.V. Hydrogen Fuel Quality Specifications for Polymer Electrolyte Fuel Cells in Road Vehicles. 2016, U.S. Department of Energy.
- [28] Jahangiri H, Bennett J, Mahjoubi P, Wilson K, Gu S. A review of advanced catalyst development for Fischer-Tropsch synthesis of hydrocarbons from biomass derived syn-gas. Catal Sci Technol 2014;4(8):2210–29.
- [29] Teimouri Z, Abatzoglou N, Dalai AK. Kinetics and Selectivity Study of Fischer-Tropsch Synthesis to C5+ Hydrocarbons. Rev Catal 2021;11(3):330. https://doi. org/10.3390/catal11030330.
- [30] Fajín, J.L.C., Cordeiro, M.N.D.S. Gomes, J.R.B. Fischer-Tropsch Synthesis on Multicomponent Catalysts: What Can We Learn from Computer Simulations? Catalysts; 2015. 5(1)
- [31] Fajín JLC, Gomes JRB, Cordeiro MNDS. Mechanistic Study of Carbon Monoxide Methanation over Pure and Rhodium- or Ruthenium-Doped Nickel Catalysts. J Phys Chem C 2015;119(29):16537–51.
- [32] Jafari R, Sotudeh-Gharebagh R, Mostoufi N. Modular Simulation of Fluidized Bed Reactors. Chem Eng Technol 2004;27(2):123–9.
- [33] Hashemi Sohi A, Eslami A, Sheikhi A, Sotudeh-Gharebagh R. Sequential-Based Process Modeling of Natural Gas Combustion in a Fluidized Bed Reactor. Energy Fuels 2012;26(4):2058–67.
- [34] Rafati M, Hashemisohi A, Wang L, Shahbazi A. Sequential Modular Simulation of Hydrodynamics and Reaction Kinetics in a Biomass Bubbling Fluidized-Bed Gasifier Using Aspen Plus. Energy Fuels 2015;29(12):8261–72.
- [35] Rafati M, Wang L, Dayton DC, Schimmel K, Kabadi V, Shahbazi A. Technoeconomic analysis of production of Fischer-Tropsch liquids via biomass gasification: The effects of Fischer-Tropsch catalysts and natural gas co-feeding. Energy Convers Manage 2017;133:153–66.
- [36] Ciferno, J.P. Marano, J.J. Benchmarking Biomass Gasification Technologies for Fuels, Chemicals and Hydrogen Production. 2002, National Energy Technology Laboratory (NETL).
- [37] Schuster G, Löffler G, Weigl K, Hofbauer H. Biomass steam gasification an extensive parametric modeling study. Bioresour Technol 2001;77(1):71–9.
- [38] Kunii, D. Levenspiel, O. Fluidization Engineering (Second Edition). Fluidization Engineering (Second Edition), ed. D. Kunii and O. Levenspiel. 1991, Boston: Butterworth-Heinemann.
- [39] Narváez I, Orío A, Aznar MP, Corella J. Biomass Gasification with Air in an Atmospheric Bubbling Fluidized Bed. Effect of Six Operational Variables on the Quality of the Produced Raw Gas. Ind Eng Chem Res 1996;35(7):2110–20.
- [40] Wang, M., et al., Greenhouse gases, Regulated Emissions, and Energy use in Technologies Model ® (2020 .Net). 2020, USDOE Office of Energy Efficiency and Renewable Energy (EERE).
- [41] Katofsky, R.E., The Production of Fluid Fuels from Biomass. 1993, Princeton University. p. 330.
- [42] Woolcock PJ, Brown RC. A review of cleaning technologies for biomass-derived syngas. Biomass Bioenergy 2013;52:54–84.
- [43] Bartholomew CH. Mechanisms of catalyst deactivation. Appl Catal A 2001;212(1-2):17-60.
- [44] Karn, F.S., et al., Fischer-Tropsch Synthesis. Poisoning of Iron Catalysts by H2S in Synthesis Gas. I&EC Product Research and Development; 1963. 2(1): p. 43-47.
- [45] Tsakoumis NE, Rønning M, Borg Ø, Rytter E, Holmen A. Deactivation of cobalt based Fischer-Tropsch catalysts: A review. Catal Today 2010;154(3-4):162–82.
- [46] Van Ree, R., et al., Modelling of a Biomass-Integrted-Gasifier/Combined-Cycle (BIG/CC) System with the Flowsheet Simulation Programme Aspen Plus; 1995.
- [47] Mendes D, Mendes A, Madeira LM, Iulianelli A, Sousa JM, Basile A. The water-gas shift reaction: from conventional catalytic systems to Pd-based membrane reactors—a review. Asia-Pac J Chem Eng 2010;5(1):111–37.
- [48] Ratnasamy C, Wagner JP. Water Gas Shift Catalysis. Catalysis Reviews 2009;51(3): 325–440.
- [49] Kang SC, Jun K-W, Lee Y-J. Effects of the CO/CO2 Ratio in Synthesis Gas on the Catalytic Behavior in Fischer-Tropsch Synthesis Using K/Fe–Cu–Al Catalysts. Energy Fuels 2013;27(11):6377–87.
- [50] Yao Y, Liu X, Hildebrandt D, Glasser D. Fischer-Tropsch Synthesis Using H2/CO/CO2 Syngas Mixtures over an Iron Catalyst. Ind Eng Chem Res 2011;50(19): 11002–12.

- [51] Martinelli M, Visconti CG, Lietti L, Forzatti P, Bassano C, Deiana P. CO2 reactivity on Fe–Zn–Cu–K Fischer-Tropsch synthesis catalysts with different K-loadings. Catal Today 2014:228:77–88.
- [52] Rohde, M., et al., Fischer-Tropsch synthesis with CO2-containing syngas from biomass Kinetic analysis of fixed bed reactor model experiments, in Studies in Surface Science and Catalysis, S.-E. Park, J.-S. Chang, and K.-W. Lee, Editors. 2004, Elsevier. p. 97-102.
- [53] Liu Y, Zhang C-H, Wang Yu, Li Y, Hao Xu, Bai L, et al. Effect of co-feeding carbon dioxide on Fischer-Tropsch synthesis over an iron-manganese catalyst in a spinning basket reactor. Fuel Process Technol 2008;89(3):234–41.
- [54] Cormos C-C. Evaluation of power generation schemes based on hydrogen-fuelled combined cycle with carbon capture and storage (CCS). Int J Hydrogen Energy 2011;36(5):3726–38.
- [55] McJannett J. Using physical solvent in multiple applications. Petrol Technol Ouarterly 2012.
- [56] van der Laan GP, Beenackers AACM. Intrinsic kinetics of the gas-solid Fischer-Tropsch and water gas shift reactions over a precipitated iron catalyst. Appl Catal A 2000:193(1-2):39-53.
- [57] Van der laan GP, Beenackers AACM. Kinetics and Selectivity of the Fischer-Tropsch Synthesis: A Literature Review. Catal Rev 1999;41(3-4):255–318.
- [58] van der Laan GP, Beenackers AACM. Hydrocarbon Selectivity Model for the Gas-Solid Fischer-Tropsch Synthesis on Precipitated Iron Catalysts. Ind Eng Chem Res 1999;38(4):1277-90.
- [59] Song H-S, Ramkrishna D, Trinh S, Wright H. Operating strategies for Fischer-Tropsch reactors: A model-directed study. Korean J Chem Eng 2004;21(2):308–17.
- [60] Mortensen PM, Dybkjær Ib. Industrial scale experience on steam reforming of CO2rich gas. Appl Catal A 2015;495:141–51.
- [61] Aasberg-Petersen K, Christensen TS, Stub Nielsen C, Dybkjær Ib. Recent developments in autothermal reforming and pre-reforming for synthesis gas production in GTL applications. Fuel Process Technol 2003;83(1-3):253–61.
- [62] Klaehn, J., et al., Water-Gas-Shift Membrane Reactor for High-Pressure Hydrogen Production. A comprehensive project report (FY2010 - FY2012). 2013: United States.
- [63] Macak J, Malecha J. Mathematical Model for the Gasification of Coal under Pressure. Ind Eng Chem Process Des Dev 1978;17(1):92–8.
- [64] Nexant, I., Equipment Design and Cost Estimation for Small Modular Biomass Systems, Synthesis Gas Cleanup, and Oxygen Separation Equipment; Task 1: Cost Estimates of Small Modular Systems. 2006: United States.
- [65] Jones WP, Lindstedt RP. Global reaction schemes for hydrocarbon combustion. Combust Flame 1988;73(3):233–49.
- [66] Peters, M.S., K.D. Timmerhaus, and K.D. Timmerhaus, Plant design and economics for chemical engineers. 4th ed. ed. McGraw-Hill chemical engineering series. 1991, New York: McGraw-Hill.
- [67] CEM. Chemical Engineering Magazine (CEM). 2021 [cited 2021; Available from: http://www.chemengonline.com/.
- [68] Maxwell, C. Cost Indices. 2021 14-Jul-2021 [cited 2021 07/30/2021]; Available from: https://www.toweringskills.com/financial-analysis/cost-indices/.
- [69] EPRI, Technical assessment guide (TAG) electricity supply, 1993. 1993.
- [70] Woods, M.C., et al., Cost and Performance Baseline for Fossil Energy Plants Volume 1: Bituminous Coal and Natural Gas to Electricity Final Report (Original Issue Date, May 2007) Revision 1, August 2007. 2007, National Energy Technology Laboratory: United States.
- [71] Searcy E, et al. The relative cost of biomass energy transport. Appl Biochem Biotechnol 2007;137(1):639–52.
- [72] EPA, Inventory of U.S. Greenbouse Gas Emissions and Sinks 1990-2019. 2021, United States Environmental Protection Agency.
- [73] EPA, AVERT, U.S. annual wind national marginal emission rate, year 2019 data. 2020: Washington, DC.
- [74] EIA. How much carbon dioxide is produced per kilowatthour of U.S. electricity generation? 2020 December 15, 2020 [cited 2021 07-31-2021]; Available from: https://www.eia.gov/tools/faqs/faq.php?id=74&t=11.
- [75] Craig, K.R. Mann, M.K. Cost and performance analysis of biomass-based integrated gasification combined-cycle (BIGCC) power systems. 1996, National Renewable Energy Lab., Golden, CO (United States): United States. p. Medium: ED; Size: 70 p.
- [76] Searcy E, Flynn P. The Impact of Biomass Availability and Processing Cost on Optimum Size and Processing Technology Selection. Appl Biochem Biotechnol 2009;154(1-3):92–107.
- [77] EIA. Table 5.6.A. Average Price of Electricity to Ultimate Customers by End-Use Sector, by State, May 2021 and 2020 (Cents per Kilowatthour). Electric Power Monthly 2021 08/01/2021]; Available from: https://www.eia.gov/electricity/monthly/epm\_table\_grapher.php?t=epmt\_5\_6\_a.
- [78] EIA, Gasoline and Diesel Fuel Update; 2021.
- [79] James, R.E., et al., Cost and Performance Baseline for Fossil Energy Plants Volume 1: Bituminous Coal and Natural Gas to Electricity. 2019: United States.